Dissipation of pesticides by stream biofilms is influenced by hydrological histories

Lluís Bertrans-Tubau, Yoann Menard, Isabelle Batisson, Nicolas Creusot, Nicolas Mazzella, Debora Millan-Navarro, Aurélie Moreira, Sergio Ponsá, Meritxell Abril, Lorenzo Proia, et al.

Dissipation of pesticides by stream biofilms is influenced by hydrological histories

Bertrans-Tubau, Lluís[1], Menard, Yoann[2], Batisson, Isabelle[2], Creusot, Nicolas[3], Mazzella, Nicolas[3], Millan-Navarro, Debora[3], Moreira, Aurélie[3], Morin, Soizic[3], Ponsá, Sergio[1], Abril, Meritxell[1], Proia, Lorenzo[1], Romaní, Anna M.[4], Artigas, Joan[2]

[1]BETA Technological Centre- University of Vic-Central University of Catalunya (BETA-UVic-UCC), Carretera de Roda 70. 08500.Vic, Barcelona, Spain
[2]Université Clermont Auvergne, CNRS, Laboratoire Microorganismes: Génome et Environnement (LMGE), Campus Universitaire des Cézeaux, 1 Impasse Amélie Murat. F-63000 Clermont- Ferrand, France
[3]INRAE, UR EABX, 50 avenue de Verdun. F-33612 Cestas, France
[4]Institute of Aquatic Ecology, University of Girona. Campus Montilivi. 17005. Girona, Spain

---

E-mail contact: lluis.bertrans@uvic.cat

Abstract

To evaluate the effects of hydrological variability on pesticide dissipation capacity by stream biofilms, we conducted a microcosm study. We exposed biofilms to short and frequent droughts (daily frequency), long and less frequent droughts (weekly frequency) and permanently immersed controls, prior to test their capacities to dissipate a cocktail of pesticides composed of tebuconazole, terbuthylazine, imidacloprid, glyphosate and its metabolite aminomethylphosphonic acid. A range of structural and functional descriptors of biofilms (algal and bacterial biomass, extracellular polymeric matrix (EPS) concentration, microbial respiration, phosphorus uptake and community-level physiological profiles) were measured to assess drought effects. In addition, various parameters were measured to characterise the dynamics of pesticide dissipation by biofilms in the different hydrological treatments (% dissipation, peak asymmetry, bioconcentration factor, among others). Results showed higher pesticide dissipation rates in biofilms exposed to short and frequent droughts, despite of their lower biomass and EPS concentration, compared to biofilms in immersed controls or exposed to long and less frequent droughts. High accumulation of hydrophobic pesticides (tebuconazole and terbuthylazine) was measured in biofilms despite the short exposure time (few minutes) in our open-flow microcosm approach. This research demonstrated the stream biofilms capacity to adsorb hydrophobic pesticides even in stressed drought environments.

Keywords

Microbial communities; hydrological variability; pesticide cocktail; artificial streams; pesticide dissipation

1. Introduction

Among freshwater microbial communities, benthic consortia, henceforth called biofilms, are assemblages of heterotrophic and autotrophic microorganisms (algae, fungi, bacteria, and cyanobacteria, among others) embedded in a self-produced matrix of extracellular polymeric substances (EPS) composed of polysaccharides, proteins, glycoproteins, and phospholipids, enhancing interactions among microbial cells (Battin *et al.* 2016). In streams, microbial cells can grow on hard surfaces such as cobbles and rocks, on soft surfaces (*i. e.*, leaf litter or wood) or in sediments, where they can obtain nutrients (Romaní *et al.* 2013) and organic compounds (including pesticides) (Edwards and Kjellerup 2013) from either the water column or the substratum itself. Biofilms contribute to the self-depuration capacity of stream waters, an important ecosystem service resulting from the removal of nutrients from water column (Saltarelli *et al.* 2021). Less studied is the attenuation capacity of pesticides such as diuron (Vercraene-Eairmal *et al.* 2010; Chaumet *et al.* 2019), glyphosate (Klátyik *et al.* 2017; Carles *et al.* 2019) or mixtures of pesticides (*e. g.*, mesotrione,

S-metolachlor, and nicosulfuron; Carles *et al.* 2017). Pesticide contamination is considered one of the greatest threats to freshwater ecosystems (Malaj *et al.* 2014; Bernhardt, Rosi and Gessner 2017). Agricultural activities (*i. e*., vineyards or cereal crops (Fernández *et al.* 2015; de Souza *et al.* 2020; Rydh Stenström, Kreuger and Goedkoop 2021; Bordin *et al.* 2022) modulate the quantity and mixtures of pesticides reaching surface waters (Cui *et al.* 2020). Aquatic biofilms have the ability to deal with pesticide contamination through accumulation, transformation and/or degradation processes (Lawrence *et al.* 2001; Sabater *et al.* 2007; Edwards and Kjellerup 2013). Biofilm's EPS matrix may contribute to pesticide dissipation thanks to its sorption capacity in sequestering cations, anions, apolar compounds and particles from the water phase (Schorer and Eisele 1997; Flemming and Wingender 2001).

Pesticide dissipation capacity of biofilms can be affected by global change environmental stressors, including those related to climate change (*i. e*., increased severity of flood and drought events), affecting the overall streams hydrology. Hydrological variations due to climate change and/or anthropic activities (*i. e*., irrigation or hydropeaking) can cause different frequencies and durations of drought events in streams. Hydrological variations caused by hydropeaking, generating short and frequent droughts (daily frequency, Li and Pasternack 2021), and by agricultural practices, generating longer and less frequent droughts (weekly frequency, Courcoul *et al.* 2022), are those mainly affecting rivers and streams in south-western Europe. Hydrological changes (*i. e*., drought episodes and high flow events) have been shown to be one of the most relevant stressors to biofilm structure and function (Romero *et al.* 2019). The study of droughts frequency and duration in aquatic microbial communities has been addressed in experimental manipulation in the field or using mesocosms (Colls *et al.* 2021). It has been observed that different duration and frequency of droughts decrease microbial densities and affect metabolism as occurred on extracellular enzymatic activities (Timoner *et al.* 2012; Romaní *et al.* 2013), microbial respiration (Gionchetta *et al.* 2020a), phosphorus uptake capacity (Proia, Romaní and Sabater 2017) or carbon degradation ability by microbial communities (Perujo, Romaní and Martín-Fernández 2020). It has been described that long-term drought (5 months) exposure induces metabolic changes in biofilms, increasing the degradation of recalcitrant organic matter, and enhancing the formation of EPS in sediment microbial communities (Gionchetta *et al.* 2019). Drought-related effects on biofilms may thus enhance biofilms capacity to degrade recalcitrant organic molecules, including pesticides.

Temporal water scarcity and dry conditions in freshwater ecosystems induce structural and functional adaptations in biofilms (Timoner *et al.* 2012; Feckler, Kahlert and Bundschuh 2015; Romero *et al.* 2019), such as EPS production. EPS contributes to the stability of the biofilm structure, commonly influenced by environmental changes such as temperature, nutrients availability and hydrological pressures (Flemming *et al.* 2023) as observed in several studies (Schmitt *et al.* 1995; Zhang *et al.*

2014; Gionchetta *et al.* 2019). Pesticide molecules retained in the EPS (Lubarsky *et al.* 2012; Chaumet *et al.* 2019) can be degraded by extracellular enzymes in the EPS (Flemming, Neu and Wingender 2016) or by intracellular oxidative processes (*e. g.* Krauss *et al.* 2011). Therefore, EPS is expected to enhance the capacity of biofilms to retain and degrade toxic molecules, provide structural stability, and increase their stress resistance to contaminants (Zhang *et al.* 2015). Accordingly, the importance of exploring pesticide interactions with aquatic biofilm communities and their dissipation on aquatic ecosystems is essential not only for single pesticide molecules but for complex cocktails of pesticide molecules present in the aquatic environment (Mayer *et al.* 1999; Stehle and Schulz 2015).

The main objective of this study was to investigate how modified hydrological scenarios (short droughts of high frequency and long droughts of short frequency) may affect the capacity of biofilm for pesticide dissipation. Specifically, we aim to decipher which structural (*i. e.*, biofilm and algal biomass, bacterial cell density and viability, EPS content, algal composition and diatoms viability) and functional (*i. e.*, microbial respiration, phosphorus uptake capacity and carbohydrates metabolism) changes in the autotrophic and heterotrophic components of drought-exposed biofilms could be responsible for changes in pesticide dissipation capacities. The study is methodologically addressed as environmentally realistic as possible by: i) working with a cocktail of pesticides [one fungicide (tebuconazole), two herbicides (terbuthylazine, glyphosate and its metabolite aminomethylphosphonic acid), and one insecticide (imidacloprid)] selected among the most common pesticide groups detected in European watersheds (Mohaupt *et al.* 2020); ii) the combination of different pesticide molecules can induce different responses in microbial communities due to their physicochemical properties, concentration in water and biofilm characteristics, thus modifying their toxicokinetic and toxicodynamic properties, which can affect their dissipation in the aquatic environment (Hernández, Gil and Lacasaña 2017); and iii) assessing the pesticide dissipation in a continuous open-flow approach. While most studies examine pesticides' dissipation by aquatic microbial communities in batch approaches (e. g., Carles *et al.* 2017; Rossi *et al.* 2021) and by ecotoxicological studies (*e. g.* diuron and triclosan; Proia *et al.* 2011; diuron, imazalil, prochloraz, simazine and chlorpyrifos; Romero *et al.* 2019), the novelty of this study was to assess the dissipation of a short pulse of a pesticide cocktail by biofilms in a continuous open-flow approach. Our main hypothesis is that biofilms affected by different hydrological scenarios would present specific structural and functional attributes influencing their performance to dissipate cocktails of pesticides in stream ecosystems. We specifically examined the total biofilm biomass and the specific EPS accumulation as potentially participating in the dissipation of the pesticide cocktail. We expected that biofilms with greater EPS content, specifically those exposed to longer droughts of low frequency (*e. g*. Gionchetta *et al.* 2019), would accumulate more pesticide molecules, improving their dissipation capacity. However, droughts are also expected to reduce total biofilms biomass and thus reduce the

sorption capacity for pesticides. Apart from the EPS role, microbial densities and metabolisms highly affected by droughts could potentially impair the responses of biofilm microorganisms to their functional capacities for ecosystem services, including pesticide dissipation. Our second hypothesis is that hydrophobic molecules present in the pesticide cocktail (tebuconazole and terbuthylazine, log K_{ow} = 3.70 and 3.40, respectively) are expected to accumulate more than hydrophilic molecules (glyphosate and AMPA, log K_{ow} = -3.20 and -2.17, respectively) in biofilms due to their intrinsic physicochemical differences (Bonnineau *et al.* 2021; Desiante, Minas and Fenner 2021).

2. Materials and methods

2.1. Experimental design

Nine artificial streams were setup in the laboratory to test the effect of droughts frequency and duration on stream biofilms' structure and functions, including their capacity for pesticides dissipation. These artificial streams, henceforth called microcosms, were composed by PVC channels with 1% of slope (length x width x depth = 2 x 0.014 x 0.010 m) connected with a 35 L plastic tank (upstream) and to a 20 L glass aquarium downstream (Figure 1). The system was filled with dechlorinated tap water (BRITA P1000; active carbon filter) and recirculated using a pump (New-Jet 1200, 1200 L h^{-1}). A 0.5 cm plastic mesh was placed at 5 cm from the top of the channel to reduce water turbulence inside the channel generated by the water tank release. The microcosms were exposed to 14 h light and 10 h dark cycle (EASY LED, 6800 K full spectrum, Aquatlantis) mimicking the late of Spring photoperiod. Air temperature was fixed at 18 °C.

Aquatic biofilms were grown on unglazed glass tiles fixed on concrete slabs placed during three weeks in the Veyre stream (France – 45°40'15.7''N, 3°06'57.8''E; Table S1). Biofilms were then transported to the laboratory and placed at the bottom of each microcosm and acclimated to laboratory conditions for four weeks. The water recirculating in the microcosms was renewed twice a week during the experiment to avoid nutrients depletion in the system and provide new microbial inoculum (1 L per microcosm at each water renewal) from the stream where biofilms were grown.

After the acclimatisation phase of biofilms, three different hydrological treatments were simulated in triplicate in the microcosms: a control condition with biofilms permanently immersed in water (IC), a condition with biofilms exposed to short droughts of high frequency (HF_SD = 1 day immersed + 1 day drought, daily frequency; hydropeaking scenario), and a condition with long droughts of low frequency (LF_LD: 1 week immersed + 1 week drought, weekly frequency; agriculture scenario). Sampling of water and biofilms were always performed in wet and light conditions. Water and biofilm samples were collected from each microcosm at S1 = day 14, S2 = day 28, S3 = day 42, S4 = day 45 and S5 = day 56. Biofilm samples were obtained by scrapping glass tiles and suspending

scrapped materials in 40 mL of previously filtered water (0.2 µm pore size nylon filters, Merck) from the corresponding microcosm. Structural (total biofilm biomass, extracellular polymeric substances concentration, microalgae and bacteria cell densities and viability, chlorophyll-*a* concentration) and functional (community-level physiological profiles, microbial respiration, and phosphorus uptake capacity) descriptors of biofilms were measured at each sampling time for each hydrological condition in triplicate.

After four weeks (day 44) of biofilms exposure to the three hydrological treatments, 10 mL of a cocktail of pesticides composed by terbuthylazine (TBT; 4.5 mg L^{-1}, purity >98%, CAS: 5915-41-3), tebuconazole (TBZ; 35 mg L^{-1}, purity >98%, CAS: 107534-96-3), imidacloprid (IMID; 35 mg L^{-1}, purity >98%, CAS: 138261-41-3), glyphosate (GLY; 35 mg L^{-1}, purity >98%, CAS: 1071-83-6) and its metabolite aminomethylphosphonic acid (AMPA; 35 mg L^{-1}, CAS: 171259-81-7), all of them obtained from Sigma-Aldrich (Table 1), was spiked at the top of each channel (before stream biofilms) in continuous open-flow conditions to reach effective concentrations of 8.12 µg L^{-1} (TBT) and 63.18 µg L^{-1} (TBZ, IMID, GLY, and AMPA) in the bottom of each artificial stream. The lower concentration of TBT compared to the rest of molecules in the cocktail is explained by its lower solubility in water. After the spiking, a total of 12 water samples were collected at the end of each channel (after stream biofilms) in order to quantify the mass of pesticides remaining after being in contact with stream biofilms (Figure 1). The previous day of pesticides spiking, 10 mL of a conservative tracer solution (NaCl, 5.54 g L^{-1}) was added at the top of each channel and electrical conductivity (EC) was recorded at the end of the channel to determine the hydrological characteristics (water velocity, discharge) of each microcosm following methods described in the Stream Solute Workshop (1990) (Table S2). From these hydrological data, we determined the specific sampling times to collect the 12 water samples at the end of the channels and quantify the mass of pesticides remaining (*i. e.* not accumulated or transformed by biofilms). Samples were taken at a frequency ranging from a few seconds to a few minutes, after spiking (time 0) and up to 22.5 minutes. Water samples consisted of 50 mL of non-filtered water to determine concentrations of neutral pesticides (TBT, IMID and TBZ) and 50 mL of filtered water (0.45 µm sterilized cellulose filter, Merck) to determine concentrations of GLY and AMPA. Samples were stored at -20 ºC until analyses. At the end of the experiment, three glass tiles were scrapped from each microcosm and filtered in a pre-weighted GF/F filter (Whatman) to determine concentrations of pesticides accumulated in the biofilms. Biofilms in filters were lyophilized and stored at -20 ºC until analyses of pesticides content.

Table 1. Cocktail pesticide molecules characteristics: solubility, octanol-water partition coefficient (Log K_{ow}), and dissipation time in water (DT50).

Pesticide molecule	**Solubility (mg L^{-1})**	**Log K_{ow} (partition octanol/water)**	**DT50 water phase (days)**
Tebuconazole (TBZ)	36.0	3.70	120-597

Glyphosate (GLY)	10500.0	-3.20	13.8-301
AMPA	146.6	-2.17	9.28-9.64
Terbuthylazine (TBT)	6.6	3.40	22.40
Imidacloprid (IMID)	610.0	0.57	184

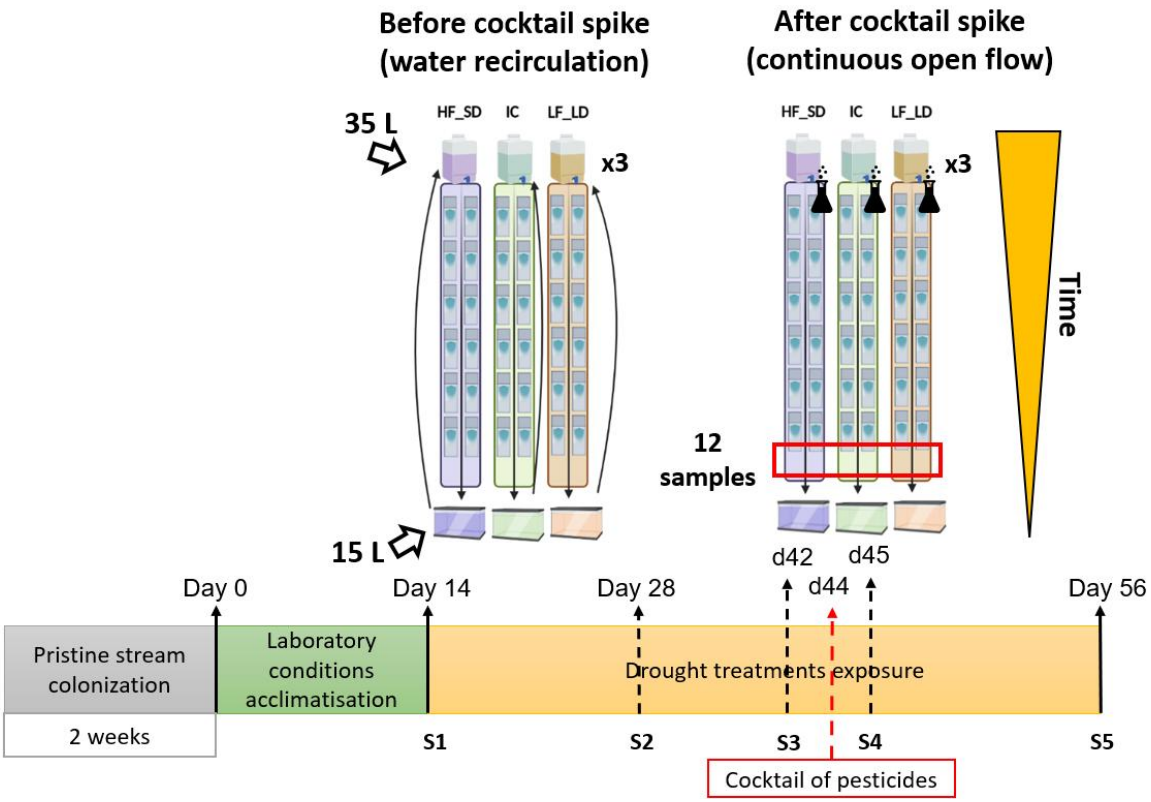

Figure 1. Experimental design of hydrological treatments before (recirculating conditions) and after (open flow conditions) the spike of the pesticide cocktail. Hydrological treatments are named as HF_SD (high frequency and short duration of drought), LF_LD (low frequency and long duration of drought), and IC (immersed control). Samples collection calendar before and after the spike of the pesticide cocktail (in red) is also represented (S1 = day 14; S2 = day 28; S3 = day 42; S4 = day 45; S5 = day 56).

2.2. Physical and chemical analyses of water

Physicochemical parameters such as electrical conductivity, dissolved oxygen concentration and saturation, water temperature (Pro DSS 4-port Digital Sampling System, YSI, U.S), light intensity (Testo 545 lux meter) and pH (FiveEasy F20, Mettler Toledo) were measured at each sampling date and microcosm. Water samples for dissolved nutrients concentration determination were previously filtered through 0.2 µm nylon filters (Merck) and analysed through spectrophotometric methods following Murphy & Riley (1962) for $P\text{-}PO_4^{3-}$ and TDP (after basic digestion) and using the $N\text{-}NO_3^-$ kit-test (Spectroquant ®, Merck). Dissolved organic carbon (DOC), total dissolved carbon (TDC),

dissolved inorganic carbon (DIC) and total dissolved nitrogen (TDN) were analysed using a TOC sampler (TOC_{VCPN}, Schimadzu, Japan).

2.3. Biofilm structural analyses

2.3.1. Bacterial density and viability

Total bacterial density (TBD) in biofilm samples was measured after sonicating twice for 60s to favour bacteria disaggregation followed by a centrifugation step at 800 *g* for 60 s. The supernatant obtained was diluted in a Tris-EDTA buffer solution x100 (1 M Tris, 0.1 M EDTA) and double stained with 100 µM SYBR Green and 1 mg mL^{-1} propidium iodide (PI) in order to distinguish live from dead bacterial cells (Invitrogen) according to Borrel *et al.* 2012. The results are given in percentage of live cells and total bacterial density (TBD) per unit of biofilm surface area in cm^2.

2.3.2. Chlorophyll-a concentration, microalgal density and total biofilm biomass

Chlorophyll-*a* concentration was measured as a proxy for algal biomass. Chlorophyll-*a* concentration was determined following Jeffrey & Humphrey (1975) using acetone 90 % as extractant. To improve pigment extraction, biofilm extracts were sonicated for 4 min at 37 KHz (Ultrasonic bath FB 1504, Fischer Scientific). The extracts were centrifuged at 800 *g* for 5 min at 6 ºC and then absorbances at 430, 665 and 750 nm were measured in the supernatant using BIOMATE 3S UV-Visible Spectrophotometer (Thermo Fisher Scientific). Chlorophyll-*a* concentrations are expressed as µg chl-*a* per cm^2.

On S5 (day 56), microalgal density was assessed using an aliquot (1 mL) from biofilm suspensions. From each homogenized subsample, 125 µL were dropped onto a Nageotte counting chamber (Marienfeld, Germany), after appropriate dilution (10 to 100-fold). Ten counting grids were randomly analysed and the number of cells of live chlorophytes, diatoms and cyanobacteria, as well as dead diatoms, were enumerated. Results were expressed as cells cm^{-2} and as percentage of diatoms viability (Morin *et al.* 2010).

Total biofilm biomass was measured from biofilm suspensions that were first centrifuged at 800 *g* during 20 min to pellet the biofilm and afterwards, dried in aluminium trays at 60 ºC for 48 h to obtain dry weight (DW) and burned at 450 ºC for 5 h to obtain ash free dry weight (AFDW) for organic and inorganic composition of biofilm. Biofilm DW and AFDW were weighted in a precision balance (PRECISA, 80A-200M, SWISS QUALITY). Results were expressed as mg AFDW cm^{-2}.

Biofilm microbial carbon (C) was calculated using conversion factors permitting to transform chlorophyll-a and bacteria to algal and bacterial carbon units. Briefly, algal biomass was calculated based on the ratio algal carbon : chlorophyll-*a* = 60 (Geider, MacIntyre and Kana 1996) and bacterial

biomass considering 2.2 x 10^{-13} g C μm^3 (Bratbak and Dundas 1984) with a mean bacterial cell biovolume of 0.1 μm^3 (Theil-Nielsen and Søndergaard 1998).

2.3.3. Extracellular polymeric substance matrix in biofilms

The concentration of glucose equivalents in the extracted extracellular polymeric substances (EPS) matrix in biofilms were measured using a cation exchange resin (CER, Dowex Marathon C sodium form, Sigma-Aldrich). CER was previously conditioned following (Romaní *et al.* 2008). Afterwards, the content of polysaccharides in the extracted biofilm EPS was measured by the phenol/H_2SO_4 – Assay (Dubois et al., 1956) at 485 nm absorption (UV-1800 spectrophotometer, Shimadzu). EPS was expressed as µg glucose-equivalent cm^{-2}.

2.4. Biofilm functional analyses

2.4.1. Community level physiological profiles (CLPP)

CLPP was tested by 96-well Biolog Ecoplates ® which produce a purple gradient response in relation to carbon substrates utilisation. Biofilm suspensions were diluted at equal densities $1x10^6$ cells mL^{-1} and inoculated to Ecoplates (150 µL per well). Plates were incubated at 22.5 °C and absorbance at 596 nm was measured every 24 h (up to 192 h) using a plate reader (Multiskan^{TM} FC Microplate Photometer, ThermoFisher Scientific). Most wells achieved sigmoid colour saturation, establishing their average well colour development (AWCD) close to 96 h. Raw absorbance data were corrected by the absorbance of the blank wells (Gionchetta *et al.* 2020b).

Different CLPP descriptors were determined at 96 h of incubation such as functional richness (S), average well colour development (AWCD), Shannon-Wiener diversity index (*H'*) and evenness (*E*) calculated as means of evaluating diversity in carbon source consumption. Additionally, kinetic parameters such as slope of AWCD, half-time to reach 50% of the slope (DT50) and β_{max} associated to the plateau level of the sigmoidal function were determined using the R package *sigmoid*. Carbon sources were divided in different groups according to Frąc et al. (2012) and Gryta et al. (2014) for further analyses (more details in Table S3).

2.4.2. Microbial respiration

Microbial respiration of biofilm communities was measured using the resazurin method according to Gionchetta *et al.* (2020a). An entire colonized glass tile from each microcosm was incubated with 100 µg L^{-1} resazurin (final concentration) in buffered pH 8 water from the corresponding microcosm. Incubations were run in the dark at 18 °C, under soft orbital shaking (40 rpm). Additionally, an abiotic sample (sterile water without biofilm) was also incubated and subtracted from biofilms respiration.

The monitoring of resazurin reduction into resorufin was performed by fluorescence measurements at two excitation/ emission wavelengths (λex 602/ λem 616; λex 570/ λem 585) on the

spectrofluorometer (SFM 25, Kontron Instruments, Italy) at 2, 4, 6, 24 and 48 h, respectively. Microbial respiration in biofilms was expressed as µg resazurin µg microbial C^{-1} $hour^{-1}$.

2.4.3. Phosphorus uptake capacity

Phosphorus uptake rate of biofilms was determined at S3 (day 42), S4 (day 45) and S5 (day 56), following the methodology described by Proia et al., (2017). We used KH_2PO_4 as stock solution to sextuplicate the background concentration of inorganic phosphate (50 µg L^{-1} to 350 µg L^{-1}, respectively) in water. An entire colonised glass tile from each microcosm was incubated for 300 min in a 100 mL flask containing dechlorinated tap water with an stream water inoculum (1:32 v:v) and the spike of the stock solution. Incubations were performed under controlled temperature (18 °C) and light conditions (14h:10h, light:dark cycle), under orbital agitation (70 rpm). Further inorganic phosphorus ($P\text{-}PO_4^{3-}$) concentrations were analysed in 5 ml water samples collected at 1, 30, 60, 90, 120, 180, 300 min after the spike of the stock solution using the Spectroquant kit-test for phosphate (Merk). An abiotic control was run in parallel to ensure a non-significant abiotic decrease in phosphorus concentration during the experiment. Phosphorus uptake was normalised by microbial carbon and time units.

2.5. Pesticide dissipation

2.5.1. Pesticides analyses

2.5.1.1. HPLC-MS/MS analysis for neutral pesticides from water and biofilm samples

Water samples for neutral pesticides (IMID, TBZ and TBT) analyses were previously filtered on Whatman® Puradisc 13 syringe filters (cellulose acetate membrane, pore size 0.45 µm), from which 1 mL was fortified at 10 ng μL^{-1} of an internal standard solution (imidacloprid d4, tebuconazole d6 and atrazine d5). The samples were further analysed through HPLC-MS/MS. For neutral pesticides in biofilm matrixes, 10 mg (dry weight) of lyophilized biofilm sample were fortified at 1 ng μL^{-1} of a surrogate solution (monuron d6, prometryn d6, simazine d5), and extracted twice on acetonitrile before evaporation in nitrogen. The resulting pellet performed a solid phase extraction (SPE) purification step by Chromabond HR-X SPE cartridges (3 mL, 60 mg, Macherey-Nagel, France) placed on a Visiprep (Supelco), conditioned initially with methanol:UPW (5mL, v/v). The final elution step was performed by flushing the cartridge with acetonitrile, previously dried under nitrogen, and fortified at 10 ng μL^{-1} of the initial solution of internal standards.

Both the neutral pesticides from water samples and biofilms were analysed with Dionex Ultimate 3000 HPLC (Thermo Fisher Scientific, Villebon-sur-Yvette, France). Chromatographic separation was performed with a Gemini-NX C18 3µm, 110 A, 100 × 2 mm with a Security Guard cartridge Gemini-NX C18 4 × 2.0 mm (Phenomenex, Le Pecq, France). Detection was performed with an API 2000 tandem mass spectrometer (Sciex, Villebon-sur-Yvette, France). Further details about mass parameters and chromatographic conditions can

be found in Lissalde *et al.* 2011, Poulier *et al.* 2021. The limits of quantification in these analyses are provided in Table S4. For further details of the chemical analysis see Supplementary material B.

2.5.1.2. HPLC-MS/MS analysis for glyphosate and AMPA from water samples

GLY and AMPA analyses were performed following the recommendations of the project ISO/DIS 16308 (Water Quality – Determination of GLY and AMPA- Method using high performance liquid chromatography (HPLC) with tandem mass spectrometry detection). The water samples were analysed by HPLC-MS/MS with the same instruments for IMID, TBZ and TBT. Reversed phase separation was performed on a X-Bridge C_{18} 3.5 µm, 2.1 x 50 mm protected by a precolumn X-Bridge C_{18} 2.1 x 10 mm (Waters, Le Pecq, France). Further details related to mass spectrometry parameter or gradient elution can be found in Fauvelle *et al.* 2015. Limits of quantification were 0.05 ng mL^{-1} for both compounds, as indicated in Table S4. Further details of the chemical analysis were detailed in Supplementary material B.

2.5.1.3. Bioconcentration factor (BCF) in biofilms

The BCF in stream biofilms at the end of the pesticide cocktail pulse was only calculated for neutral pesticide molecules (IMID, TBT and TBZ) (Wang 2016) as the ratio between the pesticide concentration in biofilms and in water (Eq.1). This factor was calculated considering both absorption and adsorption processes by biofilms. This parameter determines the capacity of biofilms to uptake the pesticide cocktail from the water column.

$$BCF = \frac{[Pesticide]_{Biofilms}}{[Pesticide]_{Water}} \ (Eq.1)$$

2.5.2. Pesticide dissipation determination by biofilms

The pesticide dissipation capacity of biofilms was measured using a mass balance approach (*e. g.* Baynes, Dix and Riviere 2012). The difference between the mass of pesticides spiked at the upper part (10 mL of the pesticide cocktail described in section 2.1) and the lower part of the channel was calculated by integrating the trapezoid area under the curve (*AUC*) resulting from the 12 water samples collected from each channel (Eq.2) (Baynes, Dix and Riviere 2012) normalised by the water flow (*Q*) (Eq.3). AUC integration of the different pesticide concentrations over time (*dt*) was obtained by *DescTools* R package. Pesticide dissipation rates (%) measured for biofilms in the three hydrological treatments were corrected by the abiotic pesticide dissipation in the microcosm system.

$$AUC = \int_0^\infty Concentration * dt \quad (Eq.2)$$

$$Q = \frac{EC\ Stock\ solution\ NaCl * Volume\ stock\ solution\ NaCl\ added}{\int_0^\infty EC * dt} \ (Eq.3)$$

Other parameters were measured in the mass balance approach to calculate the dynamics of pesticide dissipation in the different experimental treatments including: i) the peak height (in µg L^{-1}), ii) the time to rise the peak height (in seconds), and iii) the asymmetry of the peak (ratio between peak height and width). These parameters have been used to compare dissipation between hydrological treatments and pesticide molecules.

2.6. Statistical analyses

Water physicochemical characteristics (temperature, dissolved oxygen, conductivity, nutrients, among others) and biofilm descriptors (total biomass, EPS content, bacterial density and viability, chlorophyll-*a* concentration, respiration, phosphorus uptake capacity, and CLPP parameters) were compared among hydrological treatments and time by two-way repeated measures ANOVA (factor I = hydrological treatment, factor II = time). For this two-way ANOVA test we considered data from S2 to S5 and excluded S1 since hydrological treatments were not yet applied in the latter. Natural logarithm transformation was applied to all these descriptors to achieve normality and homoscedasticity of the data according to the tested factors. Post-hoc pairwise t-student p-adjusted Bonferroni's tests were performed to determine differences between hydrological treatments and time by *rstatix* R package, excepting chlorophyll-*a* concentration by Kruskal-Wallis with pairwise Wilcox tests. Moreover, microalgal densities and diatom viability measured in the last sampling day (S5) were tested through one-way ANOVA accompanied by a post-hoc test as described above, except for cyanobacteria densities which was tested through Kruskal-Wallis.

Raw CLPP data was analysed by compositional data (CoDa) following repeated measures of multivariate analysis of variance (MANOVA) (Perujo, Romaní and Martín-Fernández 2020) and the Pillai statistical test to distinguish potential functional fingerprinting differences between hydrological treatments, with graphical representation in canonical variate plots. All measured variables were first assessed by Pearson's and Spearman's correlations to check for collinearity previous to Principal Component Analysis (PCA) by *corrplot*, *FactoMineR* and *factoextra* R packages. The PCA permitted to distinguish structural and functional responses descriptors according to hydrological treatments and time effects before and after the spike of the cocktail of pesticides (S3-S4-S5).

Finally, the capacity of biofilms to dissipate the cocktail of pesticides (% of dissipation, peak height, time to reach the peak and peak asymmetry for each molecule) were compared between hydrological treatments using the non-parametric Kruskal-Wallis test with pairwise Wilcox-tests with p-adjusted of Benjamini-Hochberg (BH) in non-parametric tests (*tidyr* R package), excepted for peak asymmetry that were compared using the parametric one-way ANOVA test accompanied by Tukey test pairwise comparisons (*multcomp* and *multcompView* R package). All statistical analyses were set at 5% of significance level using RStudio version 2022.07.2+576.

3. Results

3.1. Water physicochemical characteristics

Water physicochemical parameters were monitored in the nine microcosms at each sampling date (Table S1) and showed non-significant differences between hydrological treatments (Table S5). However, time differences were observed for electrical conductivity (EC), pH, dissolved oxygen (concentration and saturation) and dissolved organic carbon (DOC) (Table S5). For instance, the percentage of oxygen saturation in water was slightly reduced from S2 to S4 and increased again at S5 independently from treatments (Table S5; Bonferroni's tests < 0.05). EC and pH showed a significant reduction after spiking the pesticide cocktail (S3 - S4) in the three treatments and recovered further at S5 (Table S5; Wilcoxon rank sum test (WRST) < 0.05). Otherwise, the average DOC concentration in all microcosms decreased progressively during the experiment from 6.9 ± 0.0 mg L^{-1} at S1 to 3.3 ± 0.7 mg L^{-1} at S5 (Table S5; Bonferroni's tests < 0.05). N-NO3, TDN, P-PO4, TDP concentrations and light did not show neither differences among hydrological treatments nor among sampling times (Table S5).

3.2. Biofilm structure in different hydrological treatments

Some biofilm structural parameters responded to hydrological treatments. Total bacterial density (TBD) in biofilms was unaffected by hydrological treatments (Figure 2.A; Table *2*), whereas the percentage of live bacterial cells were significantly lower in LF_LD compared to the other treatments (Figure 2.B; Table *2*). Those differences in the percentage of live bacterial cells were more marked at the beginning than at the end of the experiment (Figure 2.B). Otherwise, algal biomass measured as chlorophyll-*a* (Chl-*a*), microalgal density and total biofilm biomass consistently decreased in drought treatments (HF_SD and LF_LD) compared to the permanently immersed control IC (Figure 2.C and Figure S1.A; Table *2* and Table S6). Indeed, total biofilm biomass was positively correlated with Chl-*a* concentration when considering the three hydrological treatments together (Spearman coefficient = 0.7816, $p < 0.0001$).

The density of green algae was overall dominant in biofilms and droughts (HF_SD and LF_LD treatments) tended to favour green algae density over that of diatoms and cyanobacteria (Figure S1.A). The lowest Chl-*a* concentrations and total microalgal densities were measured in LF_LD compared to HF_SD and IC treatments. Surprisingly, diatoms presented low mortality despite the different hydrological treatments applied (Figure S1.B; Table S6). Extracellular polymeric substances (EPS) concentration in biofilms was also affected by droughts and strongly correlated with total biofilm biomass (Spearman coefficient = 0.75; $p < 0.0001$) (Figure 2, Table 2). Droughts drastically reduced EPS concentration in biofilms (Figure 2.D), although EPS normalised by the microbial carbon did not show differences among hydrological treatments (Figure S2; Table S7).

Some of the measured biofilm structural parameters (*i. e.*, chl-*a* concentration, percentage of live bacterial cells, and EPS concentration) varied also over time (Table *2*). While the chl-*a* concentration increased in all treatments between S2 to S5, the percentage of live bacterial cells showed an interaction between time and hydrological treatments (Table *2*). The percentage of live bacteria were significantly lower in LF_LD comparing to HF_SD and IC treatments at S2, but such differences disappeared in the other sampling dates (Figure 2.B). Moreover, the percentage of live bacteria slightly increased after spiking the pesticide cocktail from 42.59 ± 7.64% in S3 to 46.94 ± 10.55 % in S4 when considering all the treatments together (time effect: Table *2*, Bonferroni's test $P < 0.05$, Figure 2.B). Finally, EPS concentration in biofilms progressively increased over time in IC but remained rather low and stable in drought treatments (Figure 2.D).

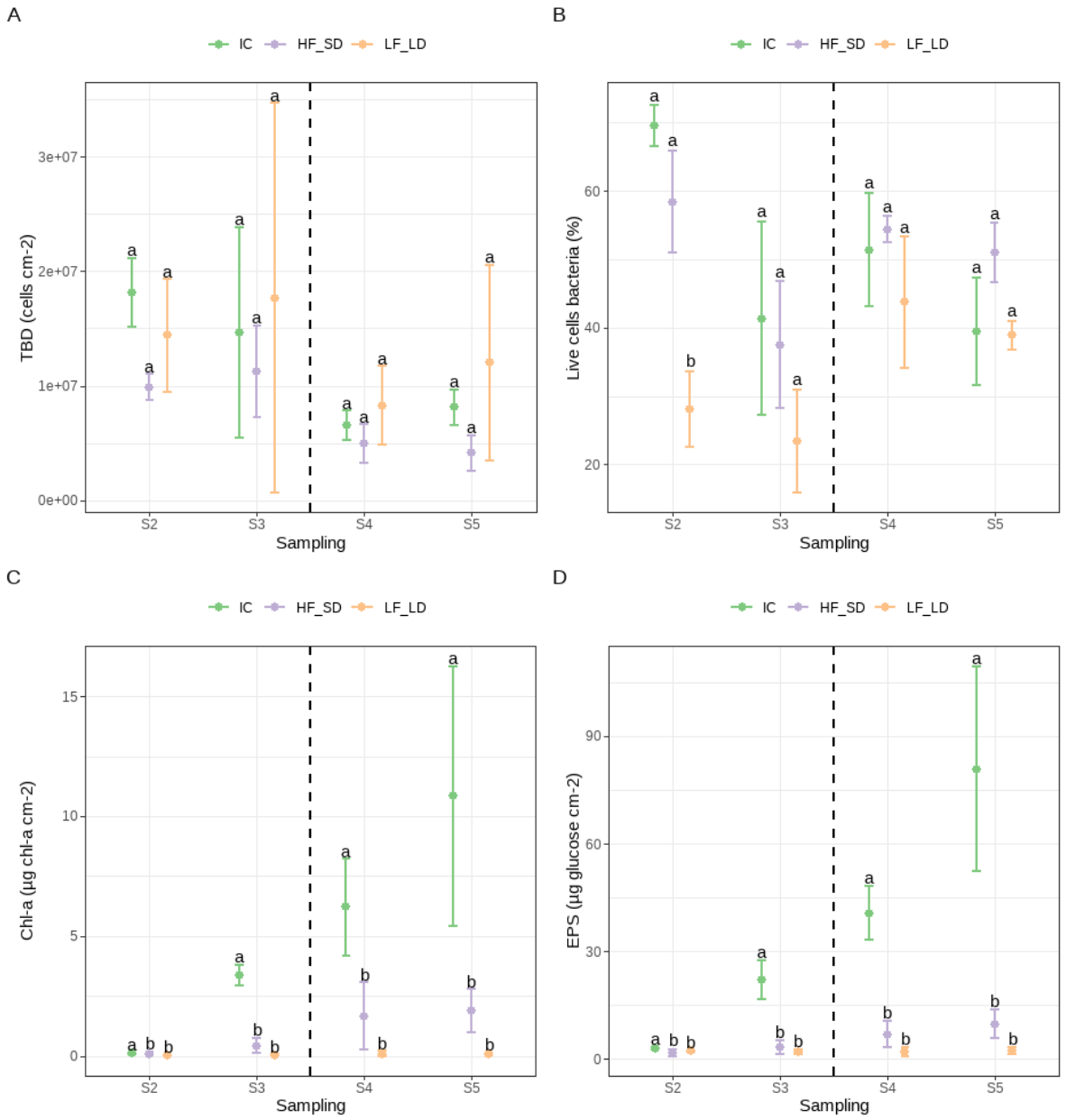

Figure 2. Total bacteria density (A), percentage of live bacteria (B), chlorophyll-a concentration (C) and EPS normalised by microbial C (D) in the three hydrological treatments (IC: immersed controls; HF_SD: high frequency and short duration drought; LF_LD: low frequency and long duration drought) in different sampling days. Different letters indicate significant differences among treatments based on Tukey post-hoc tests (descriptors A, C, D) and Wilcoxon rank-sum test (descriptor B). The dashed line represents the spike of cocktail of pesticides. Values represented are means and standard deviation (n = 3).

3.3. Biofilm function in different hydrological treatments

Biofilm respiration normalised by microbial carbon was increased by droughts. Respiration was higher in LF_LD condition, followed by HF_SD and finally the control (IC) (Figure 3.A), but at the same time, interactive effects between treatment and time were observed for respiration (Table 2).

While respiration decreased in the IC and HF_SD treatments between S2 to S5, it was maintained or even increased in the LF_LD treatment (Table 2; Bonferroni's tests < 0.05). Biofilm respiration was correlated with phosphorus (P) uptake rate when considering all the treatments together (Pearson coefficient = 0.496, p = 0.010) despite the high variability of P uptake in biofilms subjected to the LF_LD treatment (Figure 3.B). Slightly higher phosphorus uptake rate was observed in LF_LD and HF_SD compared to IC after the application of pesticides (S4 and S5), though differences between hydrological treatments were not statistically significant. P uptake capacity in biofilms slightly changed over time (Table 2).

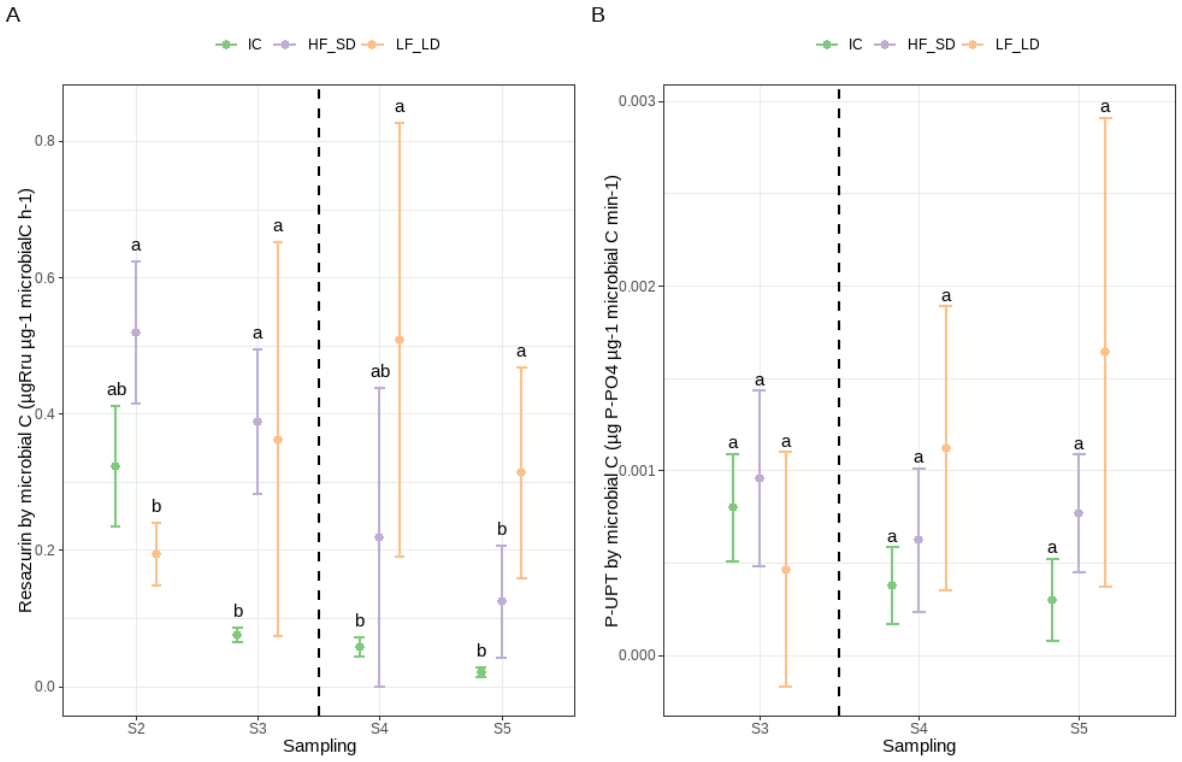

Figure 3. Microbial respiration (A) and phosphorus uptake normalised by microbial carbon (B) in the three hydrological treatments (IC: immersed controls; HF_SD: high frequency and short duration drought; LF_LD: low frequency and long duration drought) and sampling days. Different letters indicating significant differences among treatments based on Tukey post-hoc test. The dashed line represents the spike of the pesticide cocktail. Values represented are means and standard deviations (n=3).

Global community-level physiological profile (CLPP) parameters revealed that the time to dissipate 50% of substrates (DT50) showed interactive effects between hydrological treatments and time (Table *2*; Table S8). Differences were observed in HF_SD (44.34 ± 3.74 h) and LF_LD (39.72 ± 4.62 h) compared to IC (54.35 ± 5.15 h) (Table *2*; Tukey tests < 0.05) only at S4. The rest of CLPP descriptors (slope and Shannon index) were not affected by hydrological treatments but mostly by time effects (

Table *2*). In particular, higher values of the Shannon index were measured at S5 (3.06 ± 0.06) compared to S2 (2.56 ± 0.07) (Table *2*; Tukey tests < 0.05; Table S8).

When comparing the specific C substrates utilisation among hydrological treatments, a significantly lower carboxylic and ketonic acids and amines or amides catabolism, but not for amino acids catabolism, were observed in LF_LD compared to HF_SD and IC (Bonferroni tests < 0.05). Biofilm communities had major tendency to consume polymers such as α-cyclodextrin (α-Cycl) and glycogen (Glyc), and the amino acid L-asparagine(L-Asp) in LF_LD treatment (Figure 4.A), whereas D-mannitol (D-Mann), pyruvic acid methyl ester (PAME), Tween 80 (Tw80) and D-malic acid (D-MalA) is mostly consumed in the IC treatment. Finally, biofilms exposed to HF_SD mostly consumed L-serine (L-Ser), D-galactonic acid γ-lactone (D-G-Lact) and putrescine (Putr) (Figure 4.A; Table 3).

Carbon sources utilisation in biofilms did not statistically differ among sampling times compared to hydrological treatments (Figure 4.B, Table 3). Additionally, the incubation time of CLPP compositional data was embedded between 96 and 168 h (73.44 % total variance of canonical axes), excepting the compounds of tween 80 (Tw 80), i-erythritol (i-Er), putrescine (Putr), γ-hydroxybutyric acid (G-HxButA), 4-hydroxy benzoic acid (4-HxBA), β -methyl-D-glucoside (β-M-D-Gluc), D-galactonic acid γ-lactone (D-G-Lact), pyruvic acid methyl ester (PAME) and L-asparagine (L-Asp), for which the AWCD was achieved before 72 hours of incubation (Figure S3; Table S9).

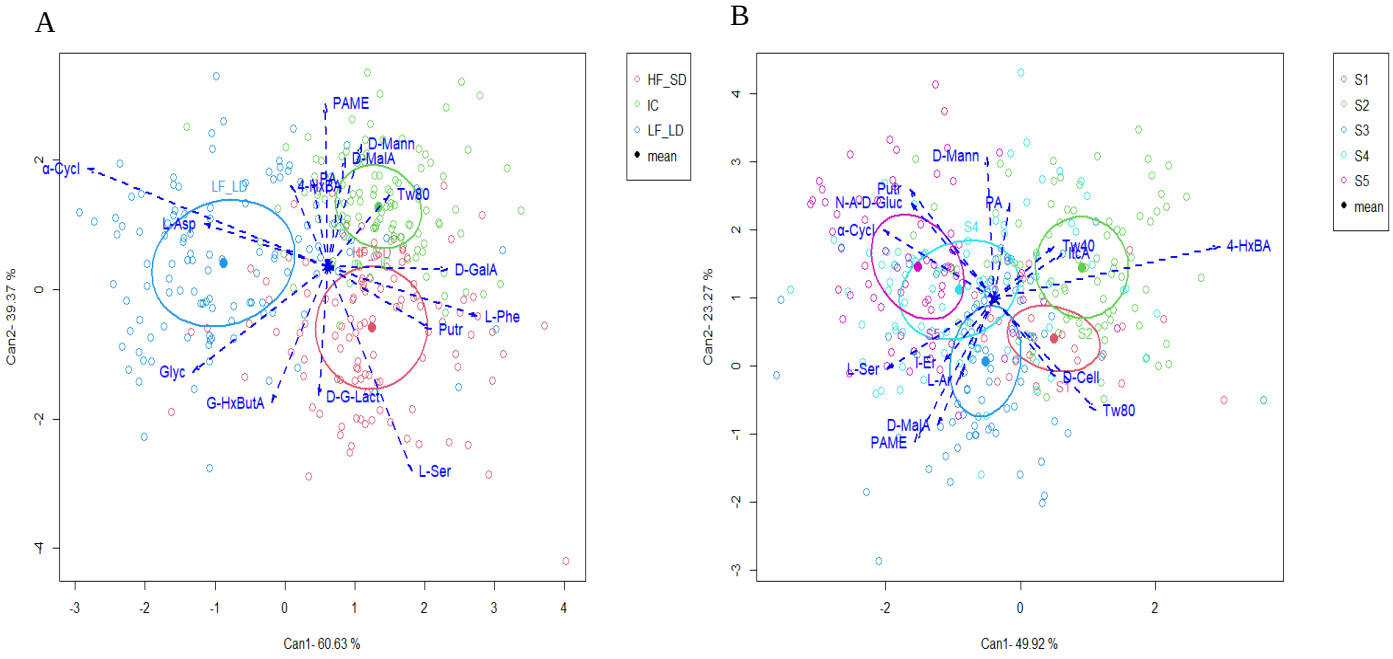

Figure 4. Canonical variates plot by hydrological treatments (A) and sampling dates (B) from CLPP canonical data.

Table 2. *Results of two-way ANOVA and χ2 and p values of Kruskal-Wallis non-parametric tests from biofilm descriptors measured in the three hydrological treatments. P-values below 0.05 are represented in bold. Chl-a = Chlorophyll-a; TBD = Total bacteria density; LC = Live cells percentage; EPS normalised by microbial C = Extracellular polymeric substance normalised by microbial carbon; Resazurin normalised by microbial C = microbial respiration by Resazurin method normalised by microbial carbon; P-UPT normalised by microbial C: Phosphorus uptake normalised by microbial carbon; Slope of AWCD: slope of average well colour development of Biolog method; DT50 of AWCD: dissipation time at 50%.*

S2-S3-S4-S5

	TWO-WAY ANOVA repeated measures			Kruskal-Wallis		
	Treatment	Time	Treatment x Time	Treatment	Time	Treatment x Time
Total biofilm biomass (mg AFDW cm^{-2}) (Ln)	**0.020 *F*=12.137**	n.s.	n.s.			
Chl-a (µg chl-a cm^{-2})				**<0.0001 χ^2=20.655**	**0.037 χ^2=8.495**	**<0.0001 χ^2=30.920**
TBD (cells cm^{-2}) (Ln)	n.s.	n.s.	n.s.			
LC (%)	**0.029 *F*=9.693**	**0.002 *F*=17.837**	**0.004 *F*=5.913**			
EPS (µg glucose cm^{-2})				**0.0001 χ^2=18.362**	**0.047 χ^2=7.949**	**0.0019 χ^2=29.426**
Resazurin by microbial C (µg Rru µg microbial C^{-1} h^{-1}) (Ln)	**0.005 *F*=26.187**	**0.013 *F*=8.864**	**0.004 *F*=6.096**			
P-UPT by microbial C (µg P-PO4 µg microbial C^{-1} min^{-1}) (Ln)*	n.s.	**0.029 *F*=32.973**	**0.006 *F*=36.607**			
Slope of AWCD (h^{-1})	n.s.	**0.020 *F*=7.274**	n.s.			
DT50 of AWCD (h)	n.s.	**0.031 *F*=5.942**	**0.029 *F*=3.547**			
Shannon diversity of AWCD	n.s.	**0.020 *F*=7.315**	n.s.			
Carbohydrates (%)	n.s.	n.s.	n.s.			
Carboxylic and ketonic acids (%)	**0.001 *F*=58.585**	**0.033 *F*=5.832**	n.s.			
Amino acids (%)	n.s.	n.s.	n.s.			
Polymers (%) (Ln)	n.s.	n.s.	n.s.			
Amines or amides (%)	**0.004 *F*=29.997**	n.s.	n.s.			

** (P-UPT only S3-S4-S5)*

Table 3. Type II Repeated Measures MANOVA Tests of CLPP and Pillai statistic tests.

	Df	Pillai test	approx F	num Df	den Df	Pr(>F)
Time	3	0.0494	0.277	3	16	n.s.
Treatment	2	0.4218	5.836	2	16	0.0125*
Time:Treatment	6	0.4042	1.809	6	16	n.s.

Signif.codes: n.s. = non-significant; (*) = significant difference (p-value < 0.05)

3.4. Relationships between biofilm structural and functional responses to hydrological treatments

The hydrological treatments clearly affected the structural and functional characteristics of biofilms (53.40 % of total explained variance in the first two dimensions of the PCA; Table S10) and separated biofilms exposed to LF_LD from those exposed to HF_SD and IC treatments (Figure 5). For instance, biofilms in the LF_LD condition presented lower microbial biomass but higher microbial respiration (*Resazurin by microbial C* in the PCA) and catabolism of polymers and carbohydrates compared to biofilms in the HF_SD and IC treatments. Biofilms in HF_SD and IC had higher algal biomass and high catabolism for amines or amides, and carboxylic and ketonic acids. Differences between HF_SD and IC biofilms were weaker, excepting for the relative abundance of live bacterial cells and amino acids catabolism that was higher in HF_SD compared to IC.

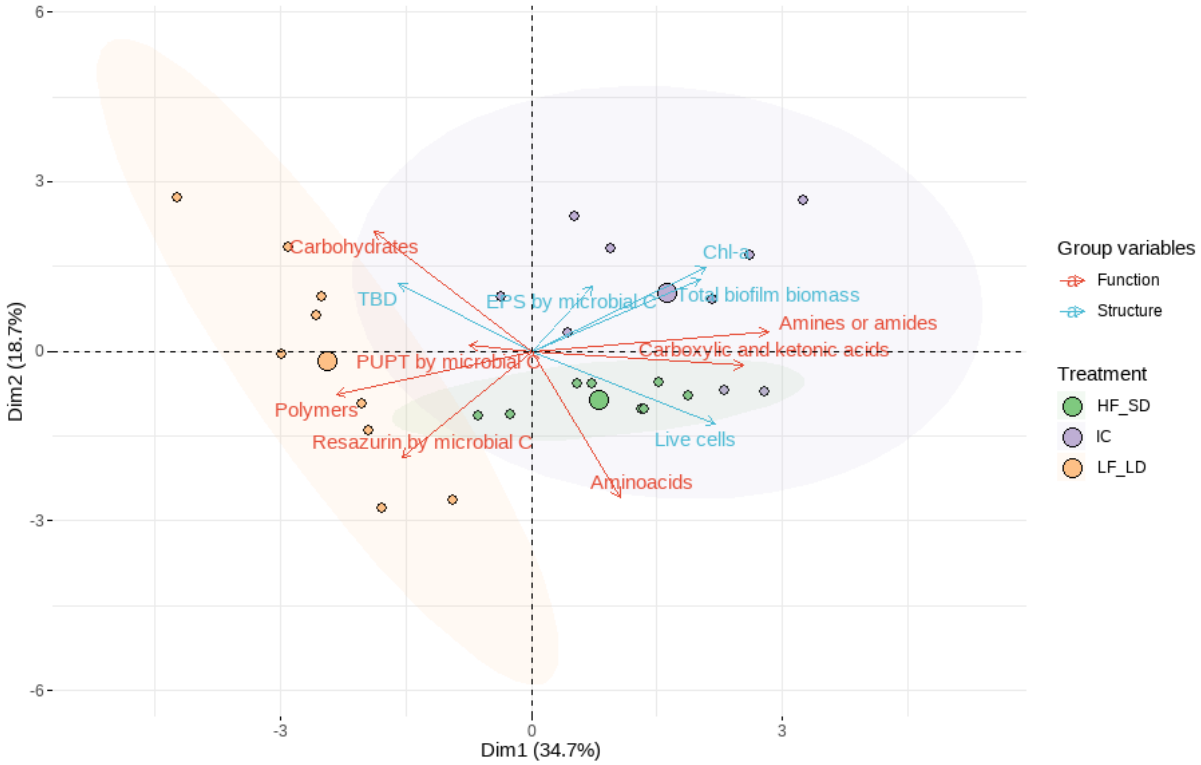

Figure 5. Principal component analysis of the structural and functional biofilm variables in the three hydrological treatments at S3, S4 and S5 of the experiment.

3.5. Pesticide dissipation capacity of biofilms

Biofilms showed an overall low capacity to dissipate the pesticide cocktail with averages of dissipation rates ranging from 2 to 35 % (imidacloprid and AMPA, respectively; Figure 6.A). However, statistical differences in pesticides dissipation among hydrological treatments were

observed ($\chi 2$= 19.681, p < 0.0001) (Figure 6.A). The dissipation percentages of the five molecules of the cocktail were generally higher in biofilms exposed to HF_SD compared to biofilms exposed to LF_LD and IC treatments (Wilcoxon rank sum test (WRST) < 0.05). When comparing the dissipation rates for each pesticide molecule separately, the lowest average dissipation percentage was measured for neutral pesticides such as imidacloprid (IMID) (8.28 ± 8.92 %), terbuthylazine (TBT) (8.57 ± 7.75 %) and tebuconazole (TBZ) (9.68 ± 8.29 %) and the highest for glyphosate (GLY) (14.00 ± 14.23 %) and its metabolite aminomethylphosphonic acid (AMPA) (16.24 ± 16.09 %), although those differences were not statistically significant (Table 4).

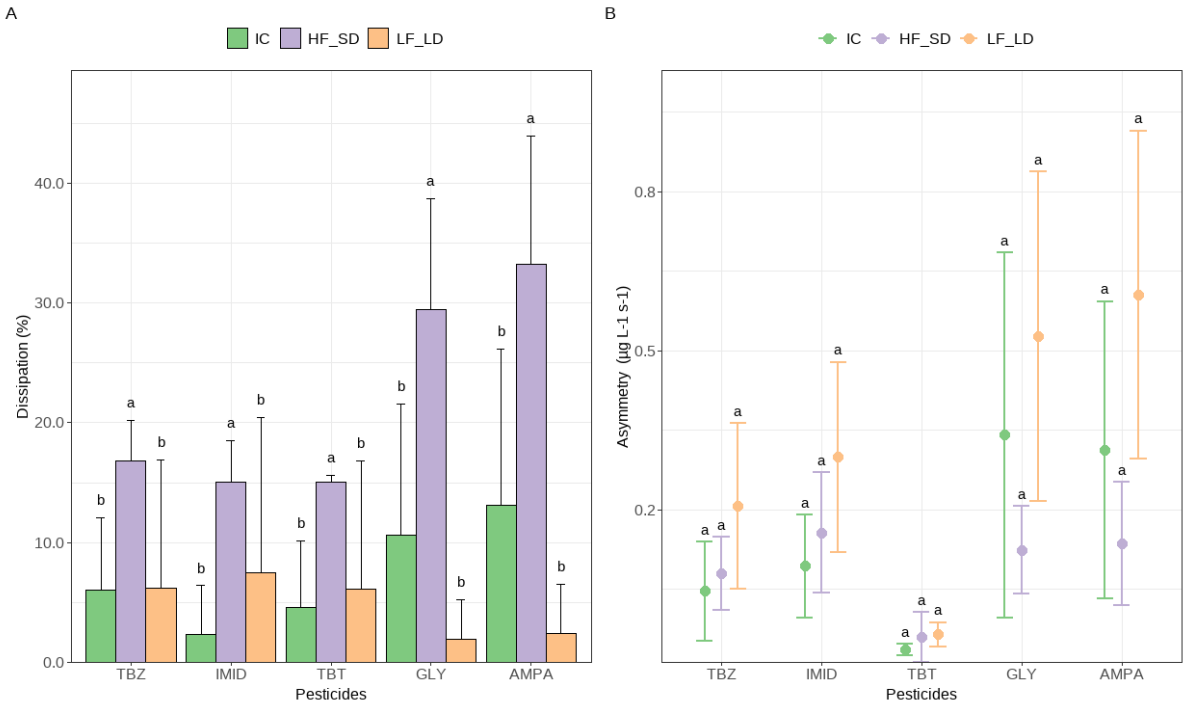

Figure 6. Dissipation rates (%) of the pesticides (AMPA = aminomethylphosphonic acid, GLY = glyphosate, IMID = imidacloprid, TBT = terbuthylazine, TBZ = tebuconazole) by biofilms exposed to different hydrological treatments (IC = immersed control, HF_SD = high frequency and short duration drought, LF_LD = low frequency and long duration drought) (A), asymmetry of pesticide peaks after the different hydrological treatments (B). Different letters indicate significant differences among treatments based on Wilcoxon rank-sum test (A) and Tukey post-hoc tests (B). Values represented are means and standard deviations (n=3).

Other toxicokinetic parameters measured during the experiment reinforced the differences in pesticides dissipation between hydrological treatments. For instance, all pesticide concentration peaks in channels were reached earlier in LF_LD (164.53 ± 31.85 s) and IC (164.53 ± 31.85 s) than in HF_SD treatments (300.67 ± 45.49 s) suggesting a greater interaction between pesticides and biofilms in the latter (Table 4; WRST < 0.05; Figure 7.A).

According to the mass balance approach of the pesticide molecules, no statistical differences in height and asymmetry of peaks for the five pesticide molecules were observed between hydrological treatments (Table 4 and Figure 7.B), though the peak asymmetry presented clear differences among pesticide molecules (F= 16.000, $p < 0.0001$). The highest peak asymmetry was measured for glyphosate and AMPA suggesting lower interaction between those molecules and the biofilms. Moreover, this peak asymmetry for GLY and AMPA was higher in LF_LD followed by IC and HF_SD treatments (Tukey tests < 0.05, Figure 6.B). Similar differences on peak asymmetry between treatments were observed for TBZ, TBT and IMID. TBT presented the lowest peak asymmetry values (0.04 ± 0.02 µg L^{-1} s^{-1}) due to the low concentration spiked compared to the other molecules from the cocktail (Tukey tests $p < 0.05$). Peak asymmetry was calculated by dividing height and width of pesticide peaks that were also significantly different among pesticide molecules (WRST < 0.05; Table 4). Peak heights of TBZ (56.46 ± 16.62 µg L^{-1}) and IMID (72.24 ± 16.19 µg L^{-1}) were lower compared to those of GLY (123.90 ± 61.00 µg L^{-1}) and AMPA (143.02 ± 66.64 µg L^{-1}) (Figure 7.A). Otherwise, peak width of GLY (411.00 ± 174.93 s) and AMPA (476.47 ± 268.28 s) were higher compared to those of TBZ (404.13 ± 211.30 s) and IMID (384.83 ± 219.33 s). The lowest peak height (8.21 ± 2.42 µg L^{-1}) and width (226.17 ± 97.88 s) were measured for TBT (Figure 7.A and Figure 7.B).

Differences in pesticides accumulation in biofilms were not observed between hydrological treatments, despite a trend of higher accumulation in the treatment LF_LD (Table 5). Differences were observed among pesticide molecules accumulation in biofilms ($\chi 2= 21.147$, $p < 0.0001$; WRST < 0.05), specifically when comparing averages of TBZ (12.30 ± 5.97 µg g^{-1} dry weight (DW) biofilm) to TBT (0.65 ± 1.67 µg g^{-1} DW biofilm) and IMID (< LOQ) in the three hydrological treatments. Despite the lower concentration of TBT in the cocktail respect to the other pesticides, this molecule tends to accumulate in biofilms together with TBZ. Accumulation of neutral pesticides (TBZ, TBT and IMID) in biofilms was highly correlated with BCF (Spearman coefficient = 0.97; $p < 0.0001$; Table 5). The highest BCF values were measured for the TBZ and TBT in LF_LD (Table 5) despite the lack of significance among hydrological treatments.

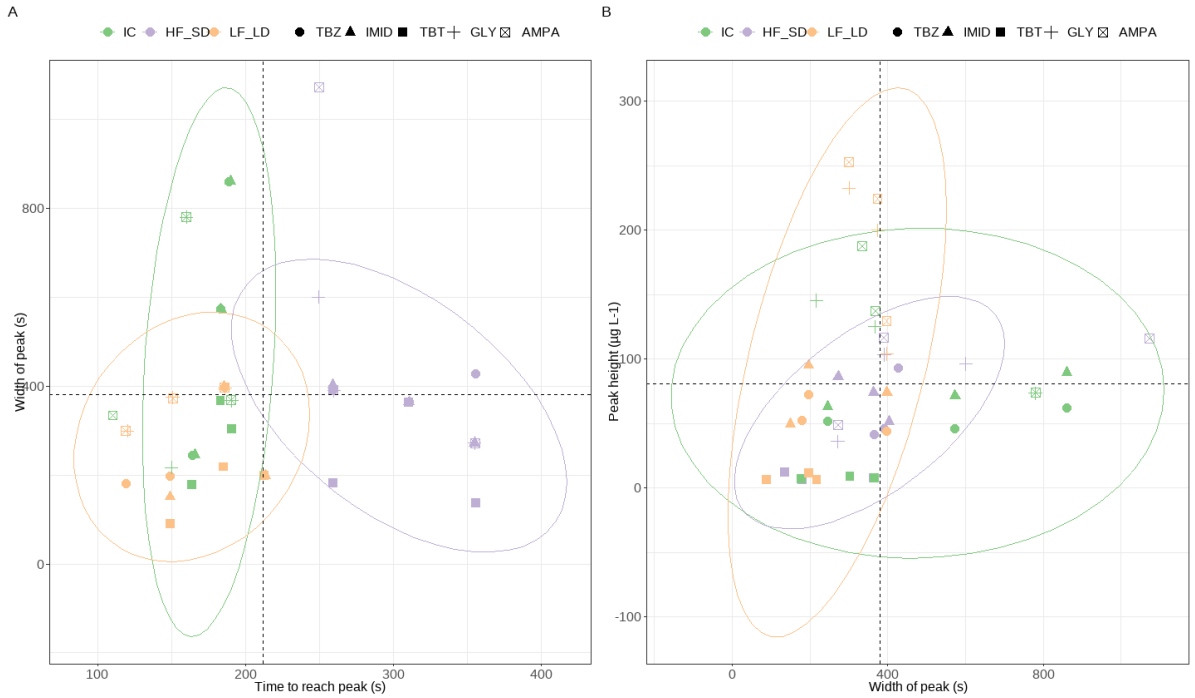

Figure 7. Pesticide peak width against time to reach the peak (A) and peak height against peak width (B) (AMPA = aminomethylphosphonic acid, GLY = glyphosate, IMID = imidacloprid, TBT = terbuthylazine, TBZ = tebuconazole) in different hydrological treatments (IC = immersed control, HF_SD = high frequency and short duration, LF_LD = low frequency and long duration) are represented.

Table 4. Results of χ2 and p values of Kruskal-Wallis non-parametric test, F and p values of one-way ANOVA. p values below 0.05 are represented in bold.

	Treatment	Pesticide
Dissipation (%)	**<0.0001 χ2=19.681**	n.s.
Peak height (µg L^{-1})	n.s.	**<0.0001 χ2=31.768**
Peak width (s)	n.s.	**0.033 χ2=10.495**
Time to reach peak (s)	**<0.0001 χ2=29.987**	n.s.
Peak asymmetry (µg L^{-1} s^{-1})	n.s.	**<0.0001 *F*=16.000**
Bioaccumulation (µg pesticide g^{-1} DW biofilm)	n.s.	**<0.0001 χ2=21.147**
BCF (L s^{-1} kg^{-1})	n.s.	**<0.0001 χ2=18.647**

Table 5. Concentration of pesticides (µg pesticide g^{-1} dry weight biofilm) and associated bioconcentration factors (BCF) (L s^{-1} kg^{-1}) of pesticides (IMID = imidacloprid, TBT = terbuthylazine, TBZ = tebuconazole) in the different hydrological treatments (IC = immersed control, HF_SD = high frequency and short duration drought, LF_LD = low frequency and long duration drought). <LOQ: under the limit of quantification (0.1 µg IMID g^{-1}biofilm extracts). Values are means ± standard deviations (n=3).

		Treatment		
	Pesticide	**Immersed control (IC)**	**High frequency and short duration drought (HF_SD)**	**Low frequency and long duration drought (LF_LD)**
Pesticide concentrations	Imidacloprid (IMID)	<LOQ (n.a.)	<LOQ (n.a.)	<LOQ (n.a.)
	Terbuthylazine (TBT)	0.12 ± 0.12	0.14 ± 0.12	1.70 ± 2.94
	Tebuconazole (TBZ)	10.61 ± 4.27	9.31 ± 7.31	16.99 ± 4.49
BCF	Imidacloprid (IMID)	<LOQ (n.a.)	<LOQ (n.a.)	<LOQ (n.a.)
	Terbuthylazine (TBT)	0.12 ± 0.13	0.11 ± 0.10	1.19 ± 2.06
	Tebuconazole (TBZ)	1.26 ± 0.13	1.08 ± 0.84	2.97 ± 1.24

n.a. (not accumulated)

4. Discussion

Drought treatments simulated in this experiment mimic the effects caused by agricultural practices and hydropeaking in rivers and streams from south-western Europe, producing different frequencies and durations of droughts that affect the structure and function of aquatic microbial communities (Acuña, Hunter and Ruhí 2017). In agricultural and urban watersheds, other stressors may affect aquatic microbial communities, such as pesticides (Dai and Dong 2014; Sharma *et al.* 2019; Meftaul *et al.* 2020; Jabiol *et al.* 2022). While loads of pesticides reaching streams are expected to decrease, pesticide concentrations in stream waters are expected to increase in watersheds subjected to droughts (Palma *et al.* 2021; Chow *et al.* 2023). Understanding how biofilm capacities to dissipate a cocktail of pesticides in streams will change in the context of climate change are of special importance for the future management of pesticide-contaminated watersheds. The present study shows that hydrological variations (long and short droughts) can modify the biofilm structure and functions, including their capacity to dissipate a cocktail of pesticides. In this section, we first addressed the specific effects of droughts on the structure and functions of biofilms (section 4.1) and then the effects of droughts on pesticide dissipation capacity by biofilms (section 4.2).

4.1. Biofilm responses to droughts

Long and short droughts applied in our experiment reduced total biofilm biomass, and especially the biomass corresponding to the autotrophic component (chlorophyll-*a* concentration, microalgal density) rather than that of the heterotrophic component (bacterial cell viability and/or total bacterial density). This result suggests that microbial autotrophs are more sensitive than microbial heterotrophs to droughts. Indeed, it has been demonstrated that aquatic microbial heterotrophic communities exposed to long drought showed higher xerotolerance, characterised by higher resistance and resilience to droughts, than autotrophic communities developed under the same treatments (Acuña *et al.* 2015). Bacterial density and cell viability did not decrease in our experiment as observed in other experiments (*i. e.*, Timoner *et al.* 2012 and Courcoul *et al.* 2022). As suggested in those studies, the run-off of dead cell debris (mostly from algal origin) in our biofilms could have been fuelling carbon and nutrients to bacteria and helping them to resist during droughts. In addition, our experiment show that green algae seem to be more resistant compared to cyanobacteria and diatoms to droughts as observed in other studies (*i. e.*, Zlatanović *et al.* 2018; Courcoul *et al.* 2022).

Various studies in the literature observed that biofilms exposed to intermittent droughts (weeks to months) became more active (*i. e*. in terms of bacterial production and extracellular enzymatic activities) compared to biofilms not exposed to droughts (Marxsen, Zoppini and Wilczek 2010; Timoner *et al.* 2014; Coulson *et al.* 2022). In our study, long droughts significantly increased biofilm respiration and modified the diversity of carbon sources utilisation. The functional responses of biofilms to droughts in our experiment were weaker than those observed in Gionchetta *et al.* 2019, Coulson *et al.* 2022 and Miao *et al.* 2023. This difference was probably explained by the short duration droughts in our experiment (from 1 day to 1 week) compared to these studies (from 5 weeks to 5 months). Regarding the shifts in carbon substrates utilisation, the increase in decomposition of polymers and carbohydrates, even carboxylic acids, by biofilms exposed to long droughts in our experiment has been already observed (Barthès *et al.* 2015). Specifically, glycogen polymers have been considered a potential resource for xerotolerant bacteria's metabolism under drought stress due to carbon accumulation in the cells (Lebre, De Maayer and Cowan 2017) and consequent decomposition, as well as carbohydrates, amines and phenolic compounds (Freixa *et al.* 2016).

Despite long droughts have been shown to favour EPS development in biofilms (Gionchetta *et al.* 2019; Coulson *et al.* 2022), contrary to our hypothesis, our results showed higher EPS content in immersed controls than in drought-exposed biofilms. This lack of EPS production in drought-exposed biofilms (both short and long droughts) could be associated with i) the short duration of droughts compared to other studies (e. g., Timoner *et al.* 2014; Gionchetta *et al.* 2019) that would have not permitted a proper EPS synthesis by microbial cells and/ or ii) the sampling strategy employed in our study, which consisted of systematic sampling under wet conditions irrespective of the drought

606 treatment, thus favouring the EPS removal when the water flow resumed. The rewetting phase, as
607 observed in Gionchetta *et al.* 2019, showed that biofilm previously exposed to drought stress reduced
608 the EPS below the permanent wet conditions, as observed in our experiment. Surprisingly, the
609 concentration of EPS increased in biofilms exposed to permanent wet conditions (IC) during the
610 length of the experiment. This result can be explained by the strong correlation observed between
611 total biofilm biomass and EPS concentration, suggesting that algal growth was probably responsible
612 for EPS production in the biofilm.

613 ## 4.2. Influence of droughts in biofilm ability to dissipate pesticides

614 Biofilms are sites for the accumulation and degradation of pesticides transported by flowing waters
615 (Rheinheimer dos Santos *et al.* 2020). It is well recognised that thicker biofilms (greater total biofilm
616 biomass) would have a stronger sorption capacity for pesticides (Guasch, Admiraal and Sabater 2003;
617 Paule *et al.* 2015). Within the biofilm components, a well-developed EPS matrix offers a physical
618 interface capable of adsorbing polar and non-polar pesticides (Fernandes *et al.* 2020). The results
619 from our study did not entirely agree with this statement, nor with our initial hypothesis, since
620 biofilms exposed to short droughts (thinner and lower EPS concentration) presented higher pesticide
621 dissipation rates, and a longer interaction time with pesticides compared to biofilms permanently
622 immersed control (thicker and higher EPS concentration). There are several possible explanations for
623 these results: i) the specific EPS quality could influence pesticides adsorption (Mahto *et al.* 2022); ii)
624 the specific functional fingerprint (greater use of carbohydrates, amino acids, amines and/or phenolic
625 compounds) could enhance developed EPS structures by increasing the cation-anion electron
626 exchange (Bonnineau *et al.* 2021) and therefore increasing their respective bioconcentration factors
627 (BCFs); ii) the increased live bacteria (after the pesticide spike, e.g., Courcoul *et al.* 2022); iii) the
628 increased dead microalgae (generating more sorption sites for pesticides, e.g., Proia *et al.* 2013); or iv)
629 other non-measured variables such as biofilm architecture (sinuosity, thickness, density and
630 viscoelasticity of the matrix, and electrostatic interactions, as observed in Battin *et al.* 2003 and
631 Flemming *et al.* 2023).

632 The accumulation of hydrophobic pesticides associated with the accumulation of microbial biomass,
633 or EPS specifically (Headley *et al.* 1998), in biofilms could explain the presence of tebuconazole and
634 terbuthylazine in biofilms from our experiment. Imidacloprid (IMID), glyphosate (GLY) and/or
635 AMPA accumulation in the biofilm was not detected and this could be explained by the lower log K_{ow}
636 of these molecules (IMID = 0.57; GLY = -3.20; AMPA = -2.17) compared to tebuconazole (TBZ =
637 3.70) and terbuthylazine (TBT = 3.40), as suggested in our initial hypothesis. The highest peak
638 asymmetry values were measured for AMPA and glyphosate, two hydrophilic molecules, highly
639 soluble in water that weakly interacted with biofilms and did not accumulate on them compared to
640 long exposure to these molecules as observed in Carles *et al.* 2019 (27 days of glyphosate exposure).

This result shows the difficulty of stream biofilms to accumulate glyphosate and AMPA molecules due to low contact time between the biofilm surface and water that could imply less capacity for biofilms to dissipate them, increasing the probability of their release to surface waters and groundwaters (Poiger *et al.* 2017). We observed tebuconazole and terbuthylazine accumulation even if the contact between biofilms and the pesticides lasted for only a few minutes in our experiment (16.38 ± 3.87 minutes). This result is in agreement with another study focused on the herbicide diuron (Chaumet *et al.* 2019) , whereas contrasts with other works in which longer exposure times were tested (48 hours to days, e.g., Romero *et al.* 2019; Courcoul *et al.* 2022). Specifically, tebuconazole was accumulated 12.30 ± 5.97 µg g^{-1} DW of biofilm in different hydrological treatments in our experiment compared to the accumulation of below 0.05 µg g^{-1} DW of biofilm in Tlili, Montuelle, Bérard, & Bouchez, 2011. The different results between this experiment and our study could be explained by the exposure conditions (chronic versus acute) and concentrations spiked to biofilms (0.5 µg L^{-1} compared to 63.18 µg L^{-1}).

We did not observe differences in pesticide molecules accumulation and BCFs in biofilms among different hydrological treatments, indicating that droughts affected the overall pesticide dissipation but not the type of pesticide molecules, although higher accumulation and BCFs was observed for tebuconazole and terbuthylazine in long droughts (LF_LD) compared to the other treatments (HF_SD and IC). This results suggest that biofilms can inform us about pesticides history in stream environments, specifically for hydrophobic molecules as observed in (Mahler *et al.* 2020). Nevertheless, further research is needed to better apprehend the strong variability in BCFs observed between microcosm replicates in our study.

5. Conclusions

The realistic assessment of pesticides dissipation by stream biofilms in a continuous open-flow approach revealed relatively low dissipation percentages per molecule in the cocktail (2 to 35 %) which should be considered specific to the type of biofilm used and the composition and concentrations of the pesticides applied. Strikingly, the capacity of stream biofilms to dissipate pesticides performed better in a drought-stressed environment subjected to short and frequent droughts compared to an environment subjected to longer droughts or permanently immersed. The continuous open-flow exposure in our experiment suggests that mostly physicochemical interactions between pesticides and biofilms occurred rather than transformation and/or degradation processes of the pesticide molecules. Contrary to our hypotheses, neither biofilm thickness nor EPS concentration were related to an enhancement of pesticide dissipation by biofilms. Other biofilm characteristics such as sinuosity, thickness or matrix density, EPS quality, and specific functional fingerprints need to be

further investigated to improve understanding on the role of biofilms in controlling pesticide fluxes in contaminated streams.

Funding

This work was supported by the EC2CO program (DeCoDry project) funded by the CNRS in France. Additional funding provided to LBT by European social funding plus (FSE+) and Generalitat de Catalunya '[grant number 2022_FI_B2 00027]'. LP has received funding from the Spanish Ministry of Science and Innovation through a Ramón y Cajal contract '[RYC 2020-029829-I]'.

Acknowledgments

This work was done during Lluís Bertrans-Tubau phD in Experimental Science and Technologies at BETA-UVIC-UCC embedded in his international traineeship at LMGE (UCA) in France. I want to be grateful to LMGE teammates for their hospitality and help, and to INRAE and UdG colleagues for their contribution and support.

6. References

Acuña V, Casellas M, Corcoll N *et al.* Increasing extent of periods of no flow in intermittent waterways promotes heterotrophy. *Freshw Biol* 2015;**60**:1810–23.

Acuña V, Hunter M, Ruhí A. Managing temporary streams and rivers as unique rather than second-class ecosystems. *Biol Conserv* 2017;**211**:12–9.

Barthès A, Ten-Hage L, Lamy A *et al.* Resilience of Aggregated Microbial Communities Subjected to Drought—Small-Scale Studies. *Microb Ecol* 2015;**70**:9–20.

Battin TJ, Besemer K, Bengtsson MM *et al.* The ecology and biogeochemistry of stream biofilms. *Nat Rev Microbiol* 2016;**14**:251–63.

Battin TJ, Kaplan LA, Newbold JD *et al.* Contributions of microbial biofilms to ecosystem processes in stream mesocosms. *Nature* 2003;**426**:439–42.

Baynes RE, Dix KJ, Riviere JE. Distribution and Pharmacokinetics Models. *Pesticide Biotransformation and Disposition*. Academic Press, 2012, 117–47.

Bernhardt ES, Rosi EJ, Gessner MO. Synthetic chemicals as agents of global change. *Front Ecol Environ* 2017;**15**:84–90.

Bonnineau C, Artigas J, Chaumet B *et al.* Role of Biofilms in Contaminant Bioaccumulation and Trophic Transfer in Aquatic Ecosystems: Current State of Knowledge and Future Challenges. In: de Voogt P (ed.). *Reviews of Environmental Contamination and Toxicology Volume 253*. Cham: Springer International Publishing, 2021, 115–53.

Bordin ER, Munhoz RC, Panicio PP *et al.* Effects of environmentally relevant concentrations of atrazine and glyphosate herbicides, isolated and in mixture, on two generation of the freshwater microcrustacean Daphnia magna. *Ecotoxicology* 2022;**31**:884–96.

Borrel G, Colombet J, Robin A *et al.* Unexpected and novel putative viruses in the sediments of a deep-dark permanently anoxic freshwater habitat. *ISME J* 2012;**6**:2119–27.

Bratbak G, Dundas I. Bacterial dry matter content and biomass estimations. *Appl Environ Microbiol* 1984;**48**:755–7.

Carles L, Gardon H, Joseph L *et al.* Meta-analysis of glyphosate contamination in surface waters and dissipation by biofilms. *Environ Int* 2019;**124**:284–93.

Carles L, Rossi F, Joly M *et al.* Biotransformation of herbicides by aquatic microbial communities associated to submerged leaves. *Environ Sci Pollut Res* 2017;**24**:3664–74.

Chaumet B, Morin S, Hourtané O *et al.* Flow conditions influence diuron toxicokinetics and toxicodynamics in freshwater biofilms. *Sci Total Environ* 2019;**652**:1242–51.

Chow R, Curchod L, Davies E *et al.* Seasonal drivers and risks of aquatic pesticide pollution in drought and post-drought conditions in three Mediterranean watersheds. *Sci Total Environ* 2023;**858**:159784.

Colls M, Timoner X, Font C *et al.* Biofilm pigments in temporary streams indicate duration and severity of drying. *Limnol Oceanogr* 2021;**66(9)**:3313–26.

Coulson LE, Feldbacher E, Pitzl B *et al.* Effects of intermittent flow on biofilms are driven by stream characteristics rather than history of intermittency. *Sci Total Environ*

2022;**849**:157809.

Courcoul C, Leflaive J, Ferriol J *et al.* The sensitivity of aquatic microbial communities to a complex agricultural contaminant depends on previous drought conditions. *Water Res* 2022;**217**, DOI: 10.1016/j.watres.2022.118396.

Cui S, Hough R, Yates K *et al.* Effects of season and sediment-water exchange processes on the partitioning of pesticides in the catchment environment: Implications for pesticides monitoring. *Sci Total Environ* 2020;**698**:134228.

Dai J, Dong H. Intensive cotton farming technologies in China: Achievements, challenges and countermeasures. *F Crop Res* 2014;**155**:99–110.

Desiante WL, Minas NS, Fenner K. Micropollutant biotransformation and bioaccumulation in natural stream biofilms. *Water Res* 2021;**193**, DOI: 10.1016/j.watres.2021.116846.

Dubois M, Gilles K, Hamilton J *et al.* A Colorimetric Method for the Determination of Sugars. *Nature* 1951;**167**:350–6.

Edwards SJ, Kjellerup B V. Applications of biofilms in bioremediation and biotransformation of persistent organic pollutants, pharmaceuticals/personal care products, and heavy metals. *Appl Microbiol Biotechnol* 2013;**97**:9909–21.

Fauvelle V, Nhu-Trang T-T, Feret T *et al.* Evaluation of Titanium Dioxide as a Binding Phase for the Passive Sampling of Glyphosate and Aminomethyl Phosphonic Acid in an Aquatic Environment. *Anal Chem* 2015;**87**:6004–9.

Feckler A, Kahlert M, Bundschuh M. Impacts of contaminants on the ecological role of lotic biofilms. *Bull Environ Contam Toxicol* 2015;**95**:421–7.

Fernandes G, Bastos MC, de Vargas JPR *et al.* The use of epilithic biofilms as bioaccumulators of pesticides and pharmaceuticals in aquatic environments. *Ecotoxicology* 2020;**29**:1293–305.

Fernández D, Voss K, Bundschuh M *et al.* Effects of fungicides on decomposer communities and litter decomposition in vineyard streams. *Sci Total Environ* 2015;**533**:40–8.

Flemming H-C, van Hullebusch ED, Neu TR *et al.* The biofilm matrix: multitasking in a shared space. *Nat Rev Microbiol* 2023;**21**:70–86.

Flemming H-C, Neu TR, Wingender J. *The Perfect Slime: Microbial Extracellular Polymeric Substances (EPS)*. IWA Publishing, 2016.

Flemming HC, Wingender J. Relevance of microbial extracellular polymeric substances (EPSs) - Part I: Structural and ecological aspects. *Water Sci Technol* 2001;**43**:1–8.

Frąc M, Oszust K, Lipiec J. Community level physiological profiles (CLPP), characterization and microbial activity of soil amended with dairy sewage sludge. *Sensors* 2012;**12**:3253–68.

Freixa A, Ejarque E, Crognale S *et al.* Sediment microbial communities rely on different dissolved organic matter sources along a Mediterranean river continuum. *Limnol Oceanogr* 2016;**61**:1389–405.

Geider RJ, MacIntyre HL, Kana TM. A dynamic model of photoadaptation in phytoplankton. *Limnol Oceanogr* 1996;**41**:1–15.

765 Gionchetta G, Artigas J, Arias-Real R *et al.* Multi-model assessment of hydrological and
766 environmental impacts on streambed microbes in Mediterranean catchments. *Environ*
767 *Microbiol* 2020a;**22**:2213–29.

768 Gionchetta G, Oliva F, Menéndez M *et al.* Key role of streambed moisture and flash storms
769 for microbial resistance and resilience to long-term drought. *Freshw Biol* 2019;**64**:306–
770 22.

771 Gionchetta G, Oliva F, Romaní AM *et al.* Hydrological variations shape diversity and
772 functional responses of streambed microbes. *Sci Total Environ* 2020b;**714**:136838.

773 Gryta A, Frąc M, Oszust K. The Application of the Biolog EcoPlate Approach in
774 Ecotoxicological Evaluation of Dairy Sewage Sludge. *Appl Biochem Biotechnol*
775 2014;**174**:1434–43.

776 Guasch H, Admiraal W, Sabater S. Contrasting effects of organic and inorganic toxicants on
777 freshwater periphyton. *Aquat Toxicol* 2003;**64**:165–75.

778 Headley J V., Gandrass J, Kuballa J *et al.* Rates of sorption and partitioning of contaminants
779 in river biofilm. *Environ Sci Technol* 1998;**32**:3968–73.

780 Hernández AF, Gil F, Lacasaña M. Toxicological interactions of pesticide mixtures: an
781 update. *Arch Toxicol* 2017;**91**:3211–23.

782 Jabiol J, Chauvet E, Guérold F *et al.* The combination of chemical, structural, and functional
783 indicators to evaluate the anthropogenic impacts on agricultural stream ecosystems.
784 *Environ Sci Pollut Res* 2022;**29**:29296–313.

785 Jeffrey SW, Humphrey GF. New spectrophotometric equations for determining chlorophylls
786 a, b, c1 and c2 in higher plants, algae and natural phytoplankton. *Biochem und Physiol*
787 *der Pflanz* 1975;**167**:191–4.

788 Klátyik S, Takács E, Mörtl M *et al.* Dissipation of the herbicide active ingredient glyphosate
789 in natural water samples in the presence of biofilms. *Int J Environ Anal Chem*
790 2017;**00**:1–21.

791 Krauss G-J, Solé M, Krauss G *et al.* Fungi in freshwaters : ecology , physiology and
792 biochemical potential. *FEMS Microbiol Rev* 2011;**35**:620–51.

793 Lebre PH, De Maayer P, Cowan DA. Xerotolerant bacteria: Surviving through a dry spell.
794 *Nat Rev Microbiol* 2017;**15**:285–96.

795 Li T, Pasternack GB. Revealing the diversity of hydropeaking flow regimes. *J Hydrol*
796 2021;**598**:126392.

797 Lissalde S, Mazzella N, Fauvelle V *et al.* Liquid chromatography coupled with tandem mass
798 spectrometry method for thirty-three pesticides in natural water and comparison of
799 performance between classical solid phase extraction and passive sampling approaches.
800 *J Chromatogr A* 2011;**1218**:1492–502.

801 Lubarsky H V., Gerbersdorf SU, Hubas C *et al.* Impairment of the bacterial biofilm stability
802 by triclosan. *PLoS One* 2012;**7**:1–16.

803 Mahler BJ, Schmidt TS, Nowell LH *et al.* Biofilms Provide New Insight into Pesticide
804 Occurrence in Streams and Links to Aquatic Ecological Communities. *Environ Sci*
805 *Technol* 2020;**54**:5509–19.

Mahto KU, Vandana M, Priyadarshanee M *et al.* Bacterial biofilm and extracellular polymeric substances in the treatment of environmental pollutants: Beyond the protective role in survivability. *J Clean Prod* 2022;**379**:134759.

Malaj E, Von Der Ohe PC, Grote M *et al.* Organic chemicals jeopardize the health of freshwater ecosystems on the continental scale. *Proc Natl Acad Sci U S A* 2014;**111**:9549–54.

Marxsen J, Zoppini A, Wilczek S. Microbial communities in streambed sediments recovering from desiccation. *FEMS Microbiol Ecol* 2010;**71**:374–86.

Mayer C, Moritz R, Kirschner C *et al.* The role of intermolecular interactions: Studies on model systems for bacterial biofilms. *Int J Biol Macromol* 1999;**26**:3–16.

Meftaul IM, Venkateswarlu K, Dharmarajan R *et al.* Controversies over human health and ecological impacts of glyphosate: Is it to be banned in modern agriculture? *Environ Pollut* 2020;**263**:114372.

Miao L, Li C, Adyel TM *et al.* Effects of the Desiccation Duration on the Dynamic Responses of Biofilm Metabolic Activities to Rewetting. *Environ Sci Technol* 2023;**57**:1828–36.

Mohaupt V, Völker J, Altenburger R *et al. Pesticides in European Rivers , Lakes and Groundwaters – Data Assessment*., 2020.

Morin S, Proia L, Ricart M *et al.* Effects of a bactericide on the structure and survival of benthic diatom communities. *Vie Milieu- Life Environ* 2010;**60**:109–16.

Murphy J, Riley JP. A modified single solution method for the determination of phosphate in natural waters. *Anal Chim Acta* 1962;**27**:31–6.

Palma P, Fialho S, Lima A *et al.* Occurrence and risk assessment of pesticides in a Mediterranean Basin with strong agricultural pressure (Guadiana Basin : Southern of Portugal). *Sci Total Environ* 2021;**794**:148703.

Paule A, Lamy A, Roubeix V *et al.* Influence of the natural growth environment on the sensitivity of phototrophic biofilm to herbicide. *Environ Sci Pollut Res* 2015;**22**:8031–43.

Perujo N, Romaní AM, Martín-Fernández JA. Microbial community-level physiological profiles: Considering whole data set and integrating dynamics of colour development. *Ecol Indic* 2020;**117**:106628.

Poiger T, Buerge IJ, Bächli A *et al.* Occurrence of the herbicide glyphosate and its metabolite AMPA in surface waters in Switzerland determined with on-line solid phase extraction LC-MS/MS. *Environ Sci Pollut Res* 2017;**24**:1588–96.

Poulier G, Lissalde S, Charriau A *et al.* Can POCIS be used in Water Framework Directive (2000 / 60 / EC) monitoring networks ? A study focusing on pesticides in a French agricultural watershed. *Sci Total Environ* 2021;**497**–**498**:282–92.

Proia L, Morin S, Peipoch M *et al.* Resistance and recovery of river biofilms receiving short pulses of Triclosan and Diuron. *Sci Total Environ* 2011;**409**:3129–37.

Proia L, Romaní A, Sabater S. Biofilm phosphorus uptake capacity as a tool for the assessment of pollutant effects in river ecosystems. *Ecotoxicology* 2017;**26**:271–82.

Proia L, Vilches C, Boninneau C *et al.* Drought episode modulates the response of river biofilms to triclosan. *Aquat Toxicol* 2013;**127**:36–45.

Rheinheimer dos Santos D, Monteiro de Castro Lima JA, Paranhos Rosa de Vargas J *et al.* Pesticide bioaccumulation in epilithic biofilms as a biomarker of agricultural activities in a representative watershed. *Environ Monit Assess* 2020;**192**:381.

Romaní AM, Amalfitano S, Artigas J *et al.* Microbial biofilm structure and organic matter use in mediterranean streams. *Hydrobiologia* 2013;**719**:43–58.

Romaní AM, Fund K, Artigas J *et al.* Relevance of polymeric matrix enzymes during biofilm formation. *Microb Ecol* 2008;**56**:427–36.

Romero F, Acuña V, Font C *et al.* Effects of multiple stressors on river biofilms depend on the time scale. *Sci Rep* 2019;**9**:1–12.

Rossi F, Carles L, Donnadieu F *et al.* Glyphosate-degrading behavior of five bacterial strains isolated from stream biofilms. *J Hazard Mater* 2021;**420**:126651.

Rydh Stenström J, Kreuger J, Goedkoop W. Pesticide mixture toxicity to algae in agricultural streams – Field observations and laboratory studies with in situ samples and reconstituted water. *Ecotoxicol Environ Saf* 2021;**215**, DOI: 10.1016/j.ecoenv.2021.112153.

Saltarelli WA, Cunha DGF, Freixa A *et al.* Nutrient stream attenuation is altered by the duration and frequency of flow intermittency. *Ecohydrology* 2021:1–11.

Schmitt J, Nivens D, White DC *et al.* Changes of biofilm properties in response to sorbed substances - an FTIR-ATR study. *Water Sci Technol* 1995;**32**:149–55.

Schorer M, Eisele M. Accumulation of inorganic and organic pollutants by biofilms in the aquatic environment. *Water, Air, Soil Pollut* 1997;**99**:651–9.

Sharma A, Kumar V, Shahzad B *et al.* Worldwide pesticide usage and its impacts on ecosystem. *SN Appl Sci* 2019;**1**:1–16.

de Souza RM, Seibert D, Quesada HB *et al.* Occurrence, impacts and general aspects of pesticides in surface water: A review. *Process Saf Environ Prot* 2020;**135**:22–37.

Stehle S, Schulz R. Agricultural insecticides threaten surface waters at the global scale. *Proc Natl Acad Sci U S A* 2015;**112**:5750–5.

Theil-Nielsen J, Søndergaard M. Bacterial carbon biomass calculated from biovolumes. *Fundam Appl Limnol* 1998;**141**:195–207.

Timoner X, Acuña V, Frampton L *et al.* Biofilm functional responses to the rehydration of a dry intermittent stream. *Hydrobiologia* 2014;**727**:185–95.

Timoner X, Acuña V, Von Schiller D *et al.* Functional responses of stream biofilms to flow cessation, desiccation and rewetting. *Freshw Biol* 2012;**57**:1565–78.

Tlili A, Montuelle B, Bérard A *et al.* Impact of chronic and acute pesticide exposures on periphyton communities. *Sci Total Environ* 2011;**409**:2102–13.

Vercraene-Eairmal M, Lauga B, Saint Laurent S *et al.* Diuron biotransformation and its effects on biofilm bacterial community structure. *Chemosphere* 2010;**81**:837–43.

Wang WX. Bioaccumulation and Biomonitoring. *Mar Ecotoxicol Curr Knowl Futur Issues*

2016:99–119.

Workshop SS. Concepts and Methods for Assessing Solute Dynamics in Stream Ecosystems. *J North Am Benthol Soc* 1990;**9**:95–119.

Zhang P, Fang F, Chen YP *et al.* Composition of EPS fractions from suspended sludge and biofilm and their roles in microbial cell aggregation. *Chemosphere* 2014;**117**:59–65.

Zhang W, Sun J, Ding W *et al.* Extracellular matrix-associated proteins form an integral and dynamic system during Pseudomonas aeruginosa biofilm development. *Front Cell Infect Microbiol* 2015;**5**:1–10.

Zlatanović S, Fabian J, Premke K *et al.* Shading and sediment structure effects on stream metabolism resistance and resilience to infrequent droughts. *Sci Total Environ* 2018;**621**:1233–42.

Supplementary material A

Table S1. Physicochemical parameters in water from the three hydrological treatments. T= Temperature; DOperc= Dissolved oxygen percentage; DOconc= Dissolved oxygen concentration; EC = Electrical conductivity; DOC = Dissolved organic carbon; TDC = Total dissolved carbon; DIC = Dissolved inorganic carbon; TDN = Total dissolved nitrogen; N-NO_3^- = nitrogen of inorganic nitrate; TDP = Total dissolved phosphorus; P-$PO4^{3-}$= phosphorus of inorganic orthophosphate. IC: Immersed controls; HF_SD: high frequency and short duration drought; LF_LD: low frequency and long duration drought. Values represent the mean and standard deviation values of 3 replicates, excepting for the Veyre stream water (n=6).

Time	Treatment	T	DOperc	DOconc	EC	Light	pH	DOC	TDC	DIC	TDN	N-NO_3^-	TDP	P-PO_4^{3-}
		ºC	%	mg L^{-1}	µS cm^{-1}	Lux		mg L^{-1}	mg L^{-1}	mg L^{-1}	mg L^{-1}	mg L^{-1}	mg L^{-1}	mg L^{-1}
S1	HF_SD	18.60±0.26	94.40±0.15	8.81±0.04	312.07±1.63	1508.00±337.03	8.03±0.05	6.88±0.82	35.97±0.90	29.09±0.48	0.55±0.12	0.74±0.20	0.016±0.021	0.009±0.005
	IC	18.7±0.26	94.27±0.15	8.81±0.04	312.07±1.63	1508.00±337.03	8.03±0.05	6.88±0.82	35.97±0.90	29.09±0.48	0.55±0.12	0.74±0.20	0.016±0.021	0.009±0.005
	LF_LD	18.60±0.26	94.27±0.15	8.81±0.04	312.07±1.63	1508.00±337.03	8.03±0.05	6.88±0.82	35.97±0.90	29.09±0.48	0.55±0.12	0.74±0.20	0.016±0.021	0.009±0.005
S2	HF_SD	18.97±0.06	93.90±0.17	8.71±0.01	266.57±27.84	1592.33±220.04	8.08±0.05	3.72±0.29	23.49±2.79	19.77±3.05	0.93±0.09	0.82±0.28	0.008±0.007	0.005±0.000
	IC	19.07±0.12	94.10±0.10	8.71±0.02	230.67±31.33	1511.00±313.08	8.05±0.12	4.84±0.49	23.65±4.84	18.81±4.57	0.90±0.05	1.14±0.16	0.025±0.027	0.003±0.003
	LF_LD	19.00±0.00	93.53±0.21	8.66±0.01	235.00±7.01	1563.00±213.06	8.05±0.02	6.00±0.11	24.93±1.49	18.93±1.60	1.28±0.08	1.32±0.36	0.037±0.029	0.017±0.003
S3	HF_SD	18.93±0.35	92.33±0.06	8.57±0.06	291.07±11.93	1661.67±135.31	7.94±0.01	3.15±0.91	29.76±1.27	26.60±1.95	0.93±0.04	1.34±0.52	0.012±0.005	0.008±0.006
	IC	19.03±0.38	93.43±0.99	8.65±0.03	294.70±5.31	1597.00±381.09	7.93±0.06	3.65±0.56	31.27±0.84	27.63±0.41	0.68±0.30	0.69±0.55	0.009±0.002	0.005±0.003
	LF_LD	18.90±0.26	91.90±0.66	8.53±0.02	278.17±6.30	1623.00±288.17	7.94±0.01	3.72±0.53	29.36±0.51	25.64±0.43	0.96±0.17	0.97±0.17	0.012±0.006	0.004±0.002
S4	HF_SD	18.83±0.25	91.13±0.86	8.44±0.11	249.83±1.33	1554.67±115.61	7.74±0.29	2.06±1.19	22.26±0.62	20.20±0.88	0.88±0.10	0.54±0.03	0.020±0.013	0.010±0.007
	IC	18.90±0.35	91.93±0.35	8.52±0.02	245.53±5.39	1533.33±364.77	7.86±0.13	2.94±1.15	22.44±0.40	19.50±0.79	0.93±0.06	0.73±0.32	0.024±0.005	0.012±0.014
	LF_LD	18.83±0.21	90.10±0.80	8.36±0.07	248.57±7.69	1565.67±260.65	7.85±0.08	2.50±0.78	22.82±1.21	20.32±0.66	0.89±0.05	1.20±0.25	0.012±0.002	0.016±0.016
S5	HF_SD	18.90±0.00	94.53±0.58	8.78±0.05	321.93±10.39	1599.33±147.29	7.87±0.08	2.91±1.52	30.12±2.10	27.20±1.62	0.60±0.29	1.45±0.42	0.008±0.001	0.007±0.002
	IC	19.07±0.06	95.07±1.34	8.80±0.14	325.50±9.39	1806.67±88.51	8.01±0.05	4.27±1.21	32.40±1.16	28.12±0.78	0.71±0.47	1.07±0.14	0.006±0.001	0.015±0.006
	LF_LD	19.07±0.06	94.23±0.57	8.72±0.05	335.90±3.08	1357.00±203.16	8.07±0.02	3.14±1.22	32.26±2.09	29.13±0.99	0.89±0.22	1.10±0.10	0.010±0.001	0.011±0.008
Veyre stream water		10.30±0.00	96.37±0.14	10.79±0.01	226.60±0.00	20333.33±1366.26	7.56±0.00	0.47±0.34	20.58±0.45	20.11±0.37	1.16±0.04	0.63±0.14	0.010±0.000	0.010±0.000

Table S2. Flow rate of each microcosm and hydrological treatments (HF_SD =High frequency and short drought exposure, IC = Immersed control, LF_LD = Low frequency and long drought exposure).

Microcosm	Treatment	Q (L/s)
C1	HF_SD	0.00491
C2	IC	0.01110
C3	LF_LD	0.01926
C4	IC	0.0095
C5	LF_LD	0.01409
C6	HF_SD	0.00760
C7	HF_SD	0.00691
C8	LF_LD	0.01221
C9	IC	0.01418

Table S3. Carbon substrate codes and their respective guilds for canonical variate plots.

C substrate	C guild	C substrate code
Pyruvic Acid Methyl Ester	Carbohydrates	PAME
Tween 40	Polymers	Tw40
Tween 80	Polymers	Tw80
αCyclodextrin	Polymers	α-Cycl
Glycogen	Polymers	Glyc
D-Cellobiose	Carbohydrates	D-Cell
α-D-Lactose	Carbohydrates	α-D-Lact
β-Methyl-DGlucoside	Carbohydrates	β-M-D-Gluc
D-Xylose	Carbohydrates	D-xyl
i-Erythritol	Carbohydrates	i-Er
D-Mannitol	Carbohydrates	D-Mann
N-Acetyl-DGlucosamine	Carbohydrates	N-A-D-Gluc
DGlucosaminic Acid	Carboxylic and ketonicacids	D-GlucA
Glucose-1- Phosphate	Carbohydrates	G-1-P
D,L-αGlycerol Phosphate	Carbohydrates	D,L-α-GlyPhos
D-Galactonic Acid γ-Lactone	Carboxylic and ketonicacids	D-G-Lact
DGalacturonic Acid	Carboxylic and ketonicacids	D-GalA
2-Hydroxy Benzoic Acid	Carboxylic and ketonicacids	2-HxBA
4-Hydroxy Benzoic Acid	Carboxylic and ketonicacids	4-HxBA
γHydroxybutyric Acid	Carboxylic and ketonicacids	G-HxButA
Itaconic Acid	Carboxylic and ketonicacids	ItcA
α-Ketobutyric Acid	Carboxylic and ketonicacids	α-KetA
D-Malic Acid	Carboxylic and ketonicacids	D-MalA
L-Arginine	Amino acids	L-Ar
L-Asparagine	Amino acids	L-Asp
LPhenylalanine	Amino acids	L-Phe
L-Serine	Amino acids	L-Ser
L-Threonine	Amino acids	L-Thr
Glycyl-LGlutamic Acid	Amino acids	Glyc-L-GlutA

Phenylethylamine	Amines or amides	PA
Putrescine	Amines or amides	Putr

911

912

913 *Table S4. Limits of quantification (LOQ) for different molecules of the cocktail of pesticides.*

Pesticide	LOQ (µg L^{-1}) water samples	LOQ (µg g^{-1}) biofilm extracts
AMPA	0.05	N/A
GLY	0.05	N/A
IMID	1	0.1
TBT	0.5	0.05
TBZ	0.5	0.05

914

915 *Table S5. Results of two-way ANOVA and χ2 and p values of Kruskal-Wallis non-parametric tests on*
916 *water physical and chemical characteristics. p values below 0.05 are represented in bold. T*
917 *=Temperature; DOperc = Dissolved oxygen percentage; DOconc = Dissolved oxygen concentration;*
918 *EC= Electrical conductivity; DOC = Dissolved organic carbon; TDN = Total Dissolved Nitrogen; N-*
919 *NO_3^- = Nitrogen of nitrate; TDP = Total dissolved phosphorus; P-PO_4^{3-} = Phosphorus of*
920 *orthophosphate.*

S2-S3-S4-S5

	TWO-WAY ANOVA repeated measures			Kruskal-Wallis		
	Treatment	Time	Treatment x Time	Treatment	Time	Treatment x Time
T(ºC)	n.s.	n.s.	n.s.			
DOperc (%)	n.s.	**0.001 *F*=27.743**	n.s.			
DOconc (mg L^{-1})	n.s.	**<0.0001 *F*=29.196**	n.s.			
EC (µs cm^{-1})				n.s.	**<0.0001 $\chi2$= 28.027**	**<0.0001 $\chi2$= 31.154**
pH				n.s.	**<0.0001 $\chi2$= 16.866**	**0.01 $\chi2$= 25.007**
Light (lux)				n.s.	n.s.	n.s.
DOC (mg L^{-1})	n.s.	**0.009 *F*=10.272**	n.s.			
TDN (mg L^{-1})				n.s.	n.s.	n.s.
N-NO_3^- (mg L^{-1})	n.s.	n.s.	n.s.			
TDP (mg L^{-1})	n.s.	n.s.	n.s.			
P-PO_4^{3-} (mg L^{-1})	n.s.	n.s.	n.s.			

921

922 *Table S6. Results of different communities of microalgal densities with F and p values of one-way*
923 *ANOVA and χ2 and p values of Kruskal-Wallis non-parametric tests. p values below 0.05 are*
924 *represented in bold.*

	ONE-WAY ANOVA	Kruskal-Wallis
	Treatment	Treatment
Total live microalgal densities (cells cm^{-2}) (Ln)	**0.002 *F*=19.57**	
Live diatoms (cells cm^{-2}) (Ln)	**0.023 *F*=7.55**	
Live green algae (cells cm^{-2}) (Ln)	**0.022 *F*=7.64**	

Live cyanobacteria (cells cm^{-2})	n.s.
Diatoms mortality rate (%)	n.s.

Table S7. Results of all experimental approach with F and p values of two-way ANOVA. p values below 0.05 are represented in bold. EPS: Extracellular polymeric substances; Resazurin: microbial respiration by Resazurin method; P-UPT: Phosphorus uptake.

	S2-S3-S4-S5		
	TWO-WAY ANOVA repeated measures		
	Treatment	Time	Treatment x Time
EPS by microbial C (µg glucose µg^{-}1 microbial C) (Ln)	n.s	n.s	n.s
Resazurin (µg Rru µg-1 cm^{-2}h^{-1}) (Ln)	**0.006** ***F*=24.209**	n.s.	**0.019** ***F*=4.018**
P-UPT (µg P-PO4 µg^{-1} cm^{-2} min^{-1}) (Ln)*	**0.004** ***F*=242.040**	n.s.	**0.023** ***F*=10.155**

** (P-UPT only S3-S4-S5)*

Table S8. Mean and standard deviation of 3 replicates of different parameters of carbon sources degradation in Biolog grouped by drought conditions (HF_SD: high frequency and short droughts; LF_LD: low frequency and long droughts; IC: immersed control) and sampling times. AWCD: Average well colour development; DT50: dissipation time at 50%.

Treatment	Time	AWCD	DT50 of AWCD (h)	Shannon of AWCD
HF_SD	S2	0.45 ± 0.10	55.06 ± 3.32	2.59 ± 0.24
HF_SD	S3	0.51 ± 0.02	50.59 ± 7.52	2.62 ± 0.14
HF_SD	S4	0.54 ± 0.18	44.35 ± 3.74	2.67 ± 0.52
HF_SD	S5	0.49 ± 0.04	49.97 ± 5.64	3.02 ± 0.14
IC	S2	0.51 ± 0.03	60.81 ± 4.97	2.60 ± 0.17
IC	S3	0.57 ± 0.12	55.62 ± 8.78	2.83 ± 0.10
IC	S4	0.55 ± 0.08	54.35 ± 5.15	2.59 ± 0.19
IC	S5	0.53 ± 0.11	40.34 ± 4.29	3.13 ± 0.08
LF_LD	S2	0.45 ± 0.12	49.72 ± 4.11	2.47 ± 0.29
LF_LD	S3	0.49 ± 0.17	41.84 ± 9.19	2.50 ± 0.63
LF_LD	S4	0.43 ± 0.18	39.72 ± 4.62	2.55 ± 0.21
LF_LD	S5	0.60 ± 0.08	48.10 ± 4.96	3.03 ± 0.13

Table S9. 31 carbon sources of Biolog grouped by sampling times and hydrological conditions (HF_SD: high frequency and short drought; LF_LD: low frequency and long drought; IC: immersed control). Table S3 for details with carbon source abbreviation. Values represented by mean ± standard deviation.

Time	Treatment	PAME	Tw40	Tw80	α-Cycl	Glyc	D-Cell	α-D-Lact	β-M-D-Gluc	D-xyl	i-Er
S2	HF_SD	0.460 ± 0.229	1.233 ± 0.223	0.707 ± 0.121	0.203 ± 0.150	0.567 ± 0.482	0.270 ± 0.155	0.317 ± 0.112	0.220 ± 0.115	0.067 ± 0.083	0.050 ± 0.087
S2	IC	0.517 ± 0.140	1.507 ± 0.230	0.853 ± 0.285	0.433 ± 0.032	0.233 ± 0.098	0.500 ± 0.075	0.473 ± 0.023	0.353 ± 0.015	0.043 ± 0.075	0.140 ± 0.017
S2	LF_LD	0.250 ± 0.122	1.030 ± 0.050	0.563 ± 0.035	0.507 ± 0.320	0.657 ± 0.473	0.747 ± 0.571	0.400 ± 0.403	0.250 ± 0.236	0.153 ± 0.155	0.000 ± 0.000
S3	HF_SD	0.383 ± 0.086	1.187 ± 0.074	0.718 ± 0.161	0.255 ± 0.092	0.386 ± 0.095	0.365 ± 0.044	0.394 ± 0.071	0.342 ± 0.065	0.198 ± 0.102	0.106 ± 0.092
S3	IC	0.615 ± 0.063	1.303 ± 0.047	0.907 ± 0.299	0.367 ± 0.038	0.212 ± 0.055	0.456 ± 0.025	0.357 ± 0.075	0.319 ± 0.057	0.188 ± 0.199	0.162 ± 0.120
S3	LF_LD	0.366 ± 0.291	1.109 ± 0.331	0.716 ± 0.240	0.567 ± 0.311	1.016 ± 0.112	0.742 ± 0.430	0.681 ± 0.677	0.527 ± 0.376	0.261 ± 0.163	0.067 ± 0.058
S4	HF_SD	0.398 ± 0.295	1.205 ± 0.266	0.699 ± 0.145	0.276 ± 0.124	0.351 ± 0.206	0.476 ± 0.211	0.389 ± 0.088	0.355 ± 0.133	0.338 ± 0.154	0.121 ± 0.121
S4	IC	0.603 ± 0.098	1.192 ± 0.186	0.619 ± 0.225	0.359 ± 0.116	0.258 ± 0.174	0.447 ± 0.137	0.407 ± 0.247	0.357 ± 0.189	0.286 ± 0.126	0.202 ± 0.128
S4	LF_LD	0.260 ± 0.077	0.985 ± 0.058	0.488 ± 0.028	0.559 ± 0.304	0.947 ± 0.160	0.681 ± 0.700	0.603 ± 0.578	0.499 ± 0.409	0.370 ± 0.430	0.064 ± 0.038
S5	HF_SD	0.437 ± 0.197	1.280 ± 0.075	0.553 ± 0.156	0.453 ± 0.115	0.583 ± 0.449	0.737 ± 0.509	0.417 ± 0.117	0.323 ± 0.095	0.433 ± 0.248	0.153 ± 0.090
S5	IC	0.580 ± 0.118	1.260 ± 0.337	0.833 ± 0.203	0.380 ± 0.010	0.533 ± 0.379	0.460 ± 0.062	0.457 ± 0.107	0.593 ± 0.427	0.377 ± 0.237	0.197 ± 0.040
S5	LF_LD	0.413 ± 0.193	1.207 ± 0.298	0.610 ± 0.164	0.683 ± 0.136	0.993 ± 0.119	0.860 ± 0.740	0.740 ± 0.436	0.303 ± 0.031	0.263 ± 0.127	0.073 ± 0.029

Time	Treatment	D-Mann	N-A-D-Gluc	D-GlucA	G-1-P	D,L-α-GlyPhos	D-G-Lact	D-GalA	2-HxBA	4-HxBA	G-HxButA
S2	HF_SD	0.580 ± 0.223	0.293 ± 0.172	0.303 ± 0.180	0.137 ± 0.140	0.040 ± 0.069	0.393 ± 0.125	1.127 ± 0.185	0.080 ± 0.139	0.563 ± 0.097	1.120 ± 0.263
S2	IC	0.627 ± 0.090	0.363 ± 0.038	0.300 ± 0.263	0.050 ± 0.087	0.117 ± 0.023	0.533 ± 0.104	1.240 ± 0.280	0.243 ± 0.421	0.663 ± 0.150	0.907 ± 0.388
S2	LF_LD	0.583 ± 0.081	0.480 ± 0.401	0.350 ± 0.161	0.060 ± 0.044	0.090 ± 0.131	0.410 ± 0.121	0.963 ± 0.127	0.163 ± 0.257	0.580 ± 0.374	1.097 ± 0.531
S3	HF_SD	0.499 ± 0.031	0.337 ± 0.060	0.264 ± 0.039	0.216 ± 0.053	0.049 ± 0.020	0.433 ± 0.050	1.238 ± 0.173	0.335 ± 0.581	0.431 ± 0.022	1.283 ± 0.102
S3	IC	0.687 ± 0.168	0.327 ± 0.064	0.522 ± 0.126	0.022 ± 0.038	0.113 ± 0.040	0.337 ± 0.142	1.368 ± 0.527	0.285 ± 0.494	0.700 ± 0.428	1.180 ± 0.620

		0.611 ±	0.498 ±	0.322 ±	0.356 ±	0.115 ±	0.512 ±	0.853 ±	0.125 ±	0.313 ±	0.955 ±	
S3	LF_LD	0.331	0.355	0.129	0.328	0.133	0.366	0.318	0.109	0.178	0.289	
		0.520 ±	0.337 ±	0.396 ±	0.176 ±	0.108 ±	0.528 ±	1.172 ±	0.585 ±	0.353 ±	1.289 ±	
S4	HF_SD	0.159	0.088	0.131	0.039	0.104	0.073	0.124	0.000	0.111	0.395	
		0.557 ±	0.670 ±	0.328 ±	0.178 ±	0.117 ±	0.494 ±	1.296 ±	0.186 ±	0.579 ±	1.003 ±	
S4	IC	0.136	0.595	0.191	0.124	0.074	0.113	0.195	0.179	0.233	0.131	
		0.465 ±	0.710 ±	0.320 ±	0.078 ±	0.020 ±	0.326 ±	0.738 ±	0.000 ±	0.267 ±	0.920 ±	
S4	LF_LD	0.199	0.742	0.062	0.134	0.017	0.109	0.342	0.000	0.150	0.564	
		0.713 ±	0.397 ±	0.340 ±	0.137 ±	0.070 ±	0.797 ±	1.273 ±	0.363 ±	0.530 ±	1.387 ±	
S5	HF_SD	0.196	0.038	0.017	0.031	0.061	0.367	0.210	0.629	0.062	0.283	
		0.630 ±	0.683 ±	0.557 ±	0.177 ±	0.147 ±	0.457 ±	1.447 ±	0.000 ±	0.590 ±	1.173 ±	
S5	IC	0.180	0.582	0.185	0.152	0.078	0.121	0.242	0.000	0.056	0.440	
		0.710 ±	0.897 ±	0.317 ±	0.000 ±	0.030 ±	0.390 ±	0.527 ±	0.057 ±	0.260 ±	1.153 ±	
S5	LF_LD	0.168	0.266	0.091	0.000	0.030	0.149	0.234	0.074	0.072	0.101	

		ItcA	**α-KetA**	**D-MalA**	**L-Ar**	**L-Asp**	**L-Phe**	**L-Ser**	**L-Thr**	**Glyc-L-GlutA**	**PA**	**Putr**
		0.293 ±	0.137 ±	0.517 ±	0.580 ±	1.623 ±	0.137 ±	0.703 ±	0.080 ±	0.153 ±	0.467 ±	0.650 ±
S2	HF_SD	0.290	0.129	0.029	0.130	0.277	0.211	0.110	0.106	0.155	0.163	0.142
		0.347 ±	0.290 ±	0.623 ±	0.463 ±	1.297 ±	0.320 ±	0.573 ±	0.177 ±	0.403 ±	0.673 ±	0.627 ±
S2	IC	0.276	0.115	0.091	0.221	0.115	0.070	0.095	0.068	0.188	0.160	0.169
		0.143 ±	0.120 ±	0.590 ±	0.633 ±	1.630 ±	0.020 ±	0.510 ±	0.093 ±	0.177 ±	0.467 ±	0.303 ±
S2	LF_LD	0.223	0.120	0.290	0.101	0.256	0.035	0.226	0.114	0.198	0.153	0.091
		0.131 ±	0.193 ±	0.863 ±	0.656 ±	1.677 ±	0.214 ±	0.953 ±	0.183 ±	0.205 ±	0.504 ±	0.821 ±
S3	HF_SD	0.116	0.110	0.263	0.267	0.180	0.150	0.200	0.033	0.093	0.272	0.276
		0.158 ±	0.276 ±	0.912 ±	0.816 ±	1.869 ±	0.250 ±	0.711 ±	0.212 ±	0.251 ±	0.741 ±	0.955 ±
S3	IC	0.153	0.182	0.315	0.370	0.287	0.071	0.390	0.104	0.104	0.216	0.263
		0.142 ±	0.158 ±	0.478 ±	0.545 ±	1.338 ±	0.103 ±	0.653 ±	0.103 ±	0.163 ±	0.415 ±	0.407 ±
S3	LF_LD	0.166	0.089	0.382	0.273	0.264	0.038	0.169	0.093	0.075	0.114	0.183
		0.146 ±	0.141 ±	0.758 ±	0.495 ±	1.810 ±	0.239 ±	0.859 ±	0.199 ±	0.189 ±	0.567 ±	1.131 ±
S4	HF_SD	0.127	0.122	0.320	0.234	0.198	0.099	0.530	0.064	0.088	0.267	0.396
		0.190 ±	0.254 ±	0.988 ±	0.709 ±	1.619 ±	0.211 ±	0.592 ±	0.224 ±	0.239 ±	0.775 ±	1.132 ±
S4	IC	0.104	0.060	0.461	0.069	0.101	0.105	0.196	0.099	0.099	0.353	0.293
		0.089 ±	0.104 ±	0.384 ±	0.349 ±	1.464 ±	0.109 ±	0.575 ±	0.090 ±	0.125 ±	0.524 ±	0.421 ±
S4	LF_LD	0.123	0.044	0.365	0.068	0.408	0.100	0.337	0.047	0.054	0.335	0.114
		0.153 ±	0.097 ±	0.720 ±	0.713 ±	2.020 ±	0.243 ±	1.487 ±	0.190 ±	0.163 ±	0.713 ±	1.157 ±
S5	HF_SD	0.012	0.047	0.123	0.206	0.122	0.086	0.465	0.036	0.031	0.015	0.260
		0.260 ±	0.223 ±	1.013 ±	0.857 ±	1.517 ±	0.247 ±	0.700 ±	0.207 ±	0.243 ±	0.647 ±	1.390 ±
S5	IC	0.165	0.081	0.248	0.674	0.395	0.061	0.130	0.127	0.042	0.067	0.646
		0.147 ±	0.200 ±	0.310 ±	0.363 ±	1.580 ±	0.183 ±	0.803 ±	0.147 ±	0.237 ±	0.457 ±	0.347 ±
S5	LF_LD	0.090	0.082	0.197	0.150	0.262	0.057	0.067	0.006	0.085	0.106	0.142

Table S10. Correlation of structural and functional variables to the three first dimensions of the PCA. TBD = Total bacteria density; LC = Live cells percentage; Chl-a = Chlorophyll-a; EPS by microbial carbon (C) = Extracellular polymeric substance corrected by microbial carbon; Resazurin (Rsz) by microbial C = microbial respiration by Resazurin method corrected by microbial carbon; P-UPT by microbial C = Phosphorus uptake corrected by microbial carbon.

	Dim.1	Dim.2	Dim.3
TBD (cells cm^{-2})	-0.49	0.37	0.62
LC (%)	0.68	-0.40	-0.26
Chl-a (µg chl-a cm^{-2})	0.64	0.46	0.13
Total biofilm biomass (mg cm^{-2})	0.62	0.39	-0.13
Rsz by microbial C (µg Rsz µgmicrobial C^{-1} h^{-1})	-0.48	-0.58	-0.24
Carbohydrates (%)	-0.58	0.65	-0.12
Polymers (%)	-0.72	-0.23	-0.17
Carboxylic and ketonic acids (%)	0.78	-0.08	0.16
Amino acids (%)	0.33	-0.79	0.18
Amines or amides (%)	0.87	0.11	0.04
PUPT by microbial C (µg $P\text{-}PO_4^{3-}$ µg microbial C^{-1} min^{-1})	-0.23	0.03	-0.54
EPS by microbial C (µg glucose µg microbial C^{-1})	0.23	0.35	-0.77

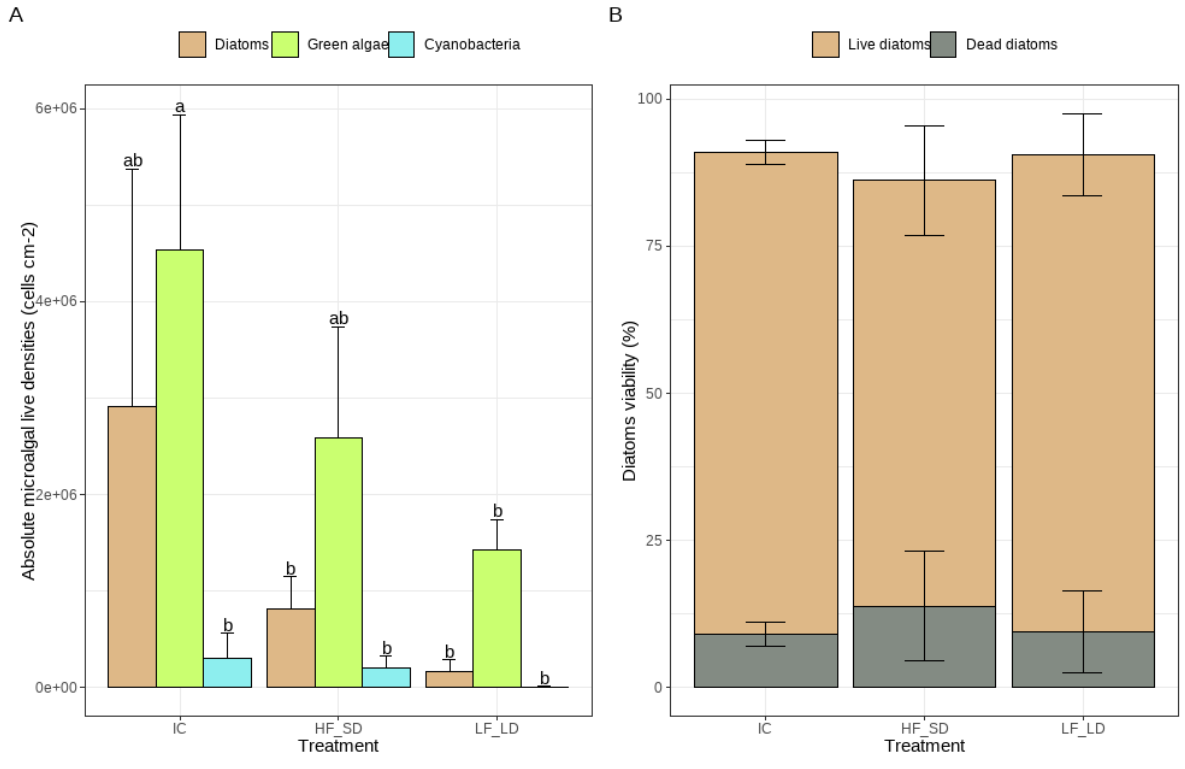

Figure S1. Absolute microalgal live densities of diatoms, green algae and cyanobacteria (A) in the last sampling time (S5) between different hydrological treatments (IC: immersed control; HF_SD: high frequency and short duration drought; LF_LD = low frequency and long duration drought) and diatoms viability rates (B). Letters represented the signification between treatments and different microalgal communities. Values ranged by mean and standard deviation.

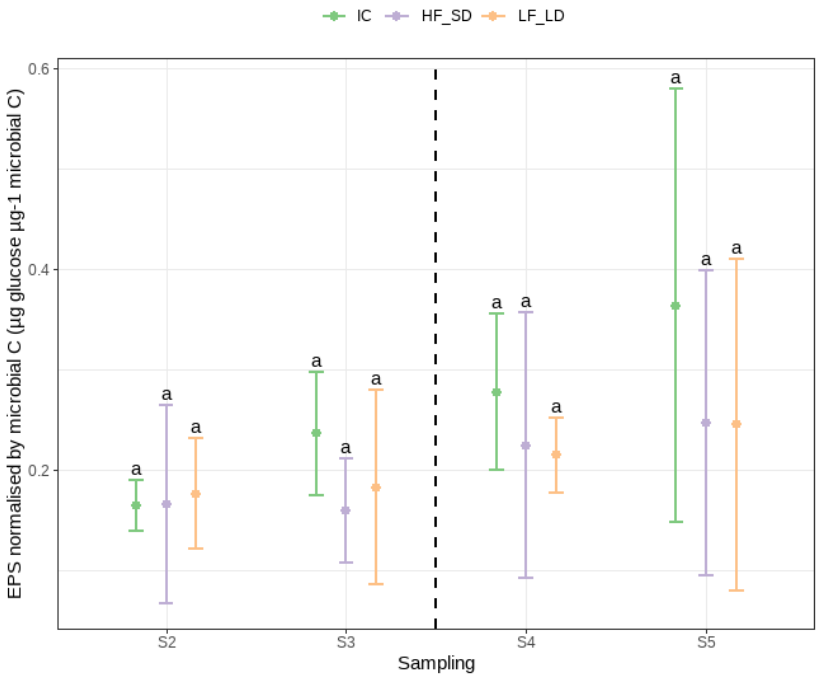

Figure S2. Extracellular polymeric substances in hydrological treatments in different sampling days. Different letters indicate significant differences among treatments based on Tukey post-hoc tests (A, C, D) and Wilcoxon rank-sum test (B). Dashed line represented the spike of cocktail of pesticides. Values represented by means and standard deviation.

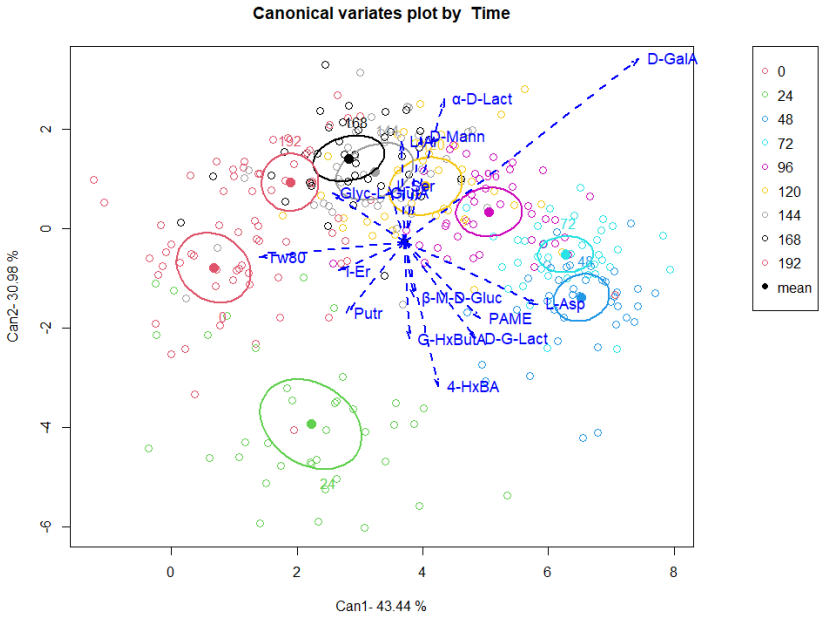

Figure S3. Canonical variates plot in function of incubation time from canonical community level physiological profile (CLPP) data.

Supplementary material B

HPLC-MS/MS analysis for neutral pesticides from water and biofilm samples

For IMID, TBZ and TBT analyses quantitation in water, 2 mL of water were filtered on Whatman® Puradisc 13 syringe filters (cellulose acetate membrane, pore size 0.45 µm). 1 mL of this filtered sample was transferred to a 1.8 mL glass vial into which 10 µL of an internal standard solution (imidacloprid d4, tebuconazole d6 and atrazine d5) at 10 ng μL^{-1} had been initially added. The samples were analysed by HPLC-MS/MS.

For the extraction of IMID, TBZ and TBT from the biofilm matrixes, 5 mL of acetonitrile were added to a 10 mL polyethylene (PE) tube containing 10 mg (dry weight) of lyophilized biofilm sample, previously conserved at -80 °C. Before extraction, 10 µL of a surrogate solution (monuron d6, prometryn d6, simazine d5) at 1 ng μL^{-1} was added to the tube. Firstly agitated, and then ultrasounded the suspension for 20 minutes. Then, 5 mL of the extract was transferred to a 15 mL glass tube to perform a second extraction with another 5 mL of acetonitrile for further evaporation under nitrogen. The resulting pellet was obtained and shaken in 10 mL of ultrapure water (UPW) before performing the solid phase extraction (SPE) purification step. Chromabond HR-X SPE cartridges (3 mL, 60 mg, Macherey-Nagel, France) were placed on a Visiprep (Supelco) and conditioned initially with 5 mL methanol (MeOH) and 5 mL UPW. The 10 mL of sample previously diluted in UPW was percolated under vacuum at a flow rate of 5 mL min^{-1}. Then, samples were rinsed with 5 mL of an UPW:MeOH (80/20, v/v) mixture. Afterwards, the cartridges were dried under nitrogen for approximately 30 minutes and stored at -20 °C until the elution step. This final elution step was performed by flushing the cartridge with 5 mL of acetonitrile. The purified extract was collected in a 15 mL glass tube which 10 µL of a solution of internal standards (imidacloprid d4, tebuconazole d6 and atrazine d5) at 10 ng μL^{-1} was also added. The sample was then evaporated to dryness under nitrogen, filled with 1 mL of UPW, and finally transferred to a 1.8 mL vial for analysis by HPLC-MS/MS.

Finally, the neutral pesticides from water samples or biofilm extracts were analysed with Dionex Ultimate 3000 HPLC (Thermo Fisher Scientific, Villebon-sur-Yvette, France). Chromatographic separation was performed with a Gemini-NX C18 3µm, 110 A, 100 × 2 mm with a Security Guard cartridge Gemini-NX C18 4 × 2.0 mm (Phenomenex, Le Pecq, France). Detection was performed with an API 2000 tandem mass spectrometer (Sciex, Villebon-sur-Yvette, France).

HPLC-MS/MS analysis for glyphosate and AMPA from water samples

The method used in this analysis followed the recommendations of the project ISO/DIS 16308 (Water Quality – Determination of GLY and AMPA- Method using high performance liquid chromatography (HPLC) with tandem mass spectrometry detection). Briefly, 5 mL of freshwater sample were

transferred into 50 mL polypropylene tubes and fortified with 50 µL of both GLY and AMPA ^{13}C, ^{15}N isotopes 20 ng mL^{-1} (surrogates). Then, 325 µL of sodium borate 50 mM and 200 µL EDTA-Na_2 0.1 M were added. The samples were homogenised and left for 5 min. 4.5 mL of acetonitrile and 600 µL of FMOC-Cl 50 mg mL^{-1} were added, and the samples were left for 30 min in the dark at room temperature (formation of FMOC derivatives). Afterwards, acetonitrile was evaporated through an azote stream during 1h approximately (until sample volume < 5 mL). Liquid-liquid extractions were then performed with addition of 3 × 1.5 mL ethyl acetate in a 15 mL graduated glass tube. The remaining ethyl acetate was removed using an azote stream for 15 min. 100 µL of formic acid 5 % was added, and the sample volume was adjusted to 5 mL and homogenised. The sample extract was then loaded onto Oasis HLB cartridges (3 mL, 60 mg, 30 µm particle size, Waters, France) after a conditioning step (1 mL MeOH followed by 1 mL formic acid 0.1 %). After sample loading, the cartridge was washed with 1 mL formic acid 0.1 % and 1 mL UPW, dried under azote, and eluted in a 1 mL graduated flask with 2 mL of ammonium hydroxide/UPW/MeOH 2:30:68 (v/v/v). The collected extract was then evaporated until the volume stabilizes at 0.5 mL. Finally, the samples volume was adjusted to 1 mL with UPW for further analysis by HPLC-MS/MS.

Analyses of both GLY and AMPA were performed by HPLC-MS/MS with the same instruments mentioned before for IMID, TBZ and TBT. Reversed phase separation was performed on a X-Bridge C_{18} 3.5 µm, 2.1 x 50 mm protected by a precolumn X-Bridge C_{18} 2.1 x 10 mm (Waters, Le Pecq, France).